International Journal of Earth Sciences (2023) 112:243–264
https://doi.org/10.1007/s00531-022-02249-3

ORIGINAL PAPER

Origin, timing and paleogeographic implications of Paleogene karst bauxites in the northern Transdanubian range, Hungary

Péter Kelemen[1,2] · István Dunkl[1] · Gábor Csillag[3,4] · Andrea Mindszenty[5] · Sándor Józsa[2] · László Fodor[3,5] · Hilmar von Eynatten[1]

Received: 10 January 2022 / Accepted: 8 September 2022 / Published online: 1 October 2022

Abstract

Paleogene karst bauxites in the northeastern Transdanubian Range and their cover sequences provide valuable sedimentary archives, despite their weathered nature and vague paleontological records. U–Pb detrital zircon geochronology combined with heavy mineral analysis indicates 'local' Alpine aeolian and fluvial sources and 'distant' aeolian sources connected to the Bohemian Massif. Records of episodic Paleogene volcanic eruptions related to igneous complexes of the Adamello and probably also the Bergell, Recsk and Balkan Peninsula, are reflected by euhedral zircon crystals. Their U–Pb geochronology supplies age constraints for the phases of subaerial exposure of the karstic surface and the accumulation of bauxitic protoliths and helps to improve the existing stratigraphic records and to define stages of denudation in the northeastern Transdanubian Range. Distinct phases of subaerial exposure and accumulation of the bauxite's protoliths are identified as ca. 42, 35 and 31 Ma; alternating with episodes of subsidence, represented by siliciclastic and carbonatic sequences at ca. 38, 32 and 31 Ma. Besides Paleogene volcanism, zircon dating also revealed contributions from the Middle Triassic tuffs of the Transdanubian Range. Garnet, epidote, kyanite, staurolite, and xenotime/monazite crystals suggest fluvial drainage of diverse metamorphic units of the Austroalpine basement from the Eastern- and Southern Alps, which also supplied most of the pre-Mesozoic zircons. However, the unexpectedly high proportion of Variscan ages in the bauxites most likely relate to igneous rocks of the Bohemian Massif, thus suggesting additional long-distance aeolian sources. The new data allow for detailed reconstructions of the Paleogene evolution and palaeogeography of the northeastern Transdanubian range.

Keywords Paleogene volcanism · Karst bauxite · Provenance · Palaeogeography · U–Pb geochronology · Transdanubian range

Introduction

The reconstruction of Earth's history intimately relies on continuous and well-dated sedimentary archives. On uplifted terrestrial areas such archives are rather limited or completely missing. In these settings, residual sediments like bauxite, terra rossa, red clay or kaolin deposits, formed as a result of discontinuous sediment accumulation and continental subaerial weathering. They represent important archives that may reveal past climate conditions, the composition and provenance of aeolian dust, volcanism, palaeorelief and local as well as far-field tectonic processes (e.g., D'Argenio and Mindszenty 1995; Wang et al. 2018; Marchand et al. 2021). However, due to the lack of biostratigraphic data, age constraints are typically scarce due to the highly weathered nature of these residual sediments. Moreover, the original petrographical and geochemical characteristics of the source

✉ Péter Kelemen
kelemenpeter1991@gmail.com

1 Department of Sedimentology and Environmental Geology, Geoscience Center, University of Göttingen, Göttingen, Germany

2 Department of Petrology and Geochemistry, Institute of Geography and Earth Sciences, Eötvös Loránd University, Budapest, Hungary

3 Department of Geology, Institute of Geography and Earth Sciences, Eötvös Loránd University, Budapest, Hungary

4 Institute for Geological and Geochemical Research, Research Centre for Astronomy and Earth Sciences, Hungarian Academy of Sciences, Budapest, Hungary

5 ELTE-MTA Geological, Geophysical and Space Science Research Group at Eötvös Loránd University, Institute of Geography and Earth Sciences, Budapest, Hungary

formations were transformed by intense weathering. Consequently, the common rock-forming silicates broke down and dissolved under subtropical to tropical wet climate conditions during surface or near-surface bauxite formation processes (e.g., Bárdossy and Aleva 1990).

In such sediments and sedimentary rocks, the occurrence of ultrastable and datable detrital mineral grains—most prominently zircon—practically offers the only way to (i) date the source rocks and (ii) constrain the maximum age of deposition (e.g., Comer et al. 1980a, b; Dunkl 1992; Kelemen et al. 2017; Marchand et al. 2021). Zircons form in a wide range of geological processes, but detrital zircons mostly represent felsic to intermediate igneous sources in sedimentary rocks (Mange and Mauer 1992). Heavy mineral analysis provides an additional tool to unravel possible igneous and metamorphic source components in bauxitic sediments. The detection and quantification of occasionally preserved heavy minerals such as tourmaline, garnet, Al-silicates, epidote and amphibole allow for acquiring a more complete picture of the source rocks and depositional setting (e.g., Comer 1974; Dennen and Norton 1977; Mindszenty et al. 1991; Wang et al. 2012; Kelemen et al. 2017, 2021).

The Transdanubian Range (TR) in western Hungary represents the structurally highest tectonic unit in the Eastern Alps—Western Carpathians (Fig. 1; Tari 1994; Schmid et al. 2008; Tari and Horváth 2010). The Mesozoic and Paleogene

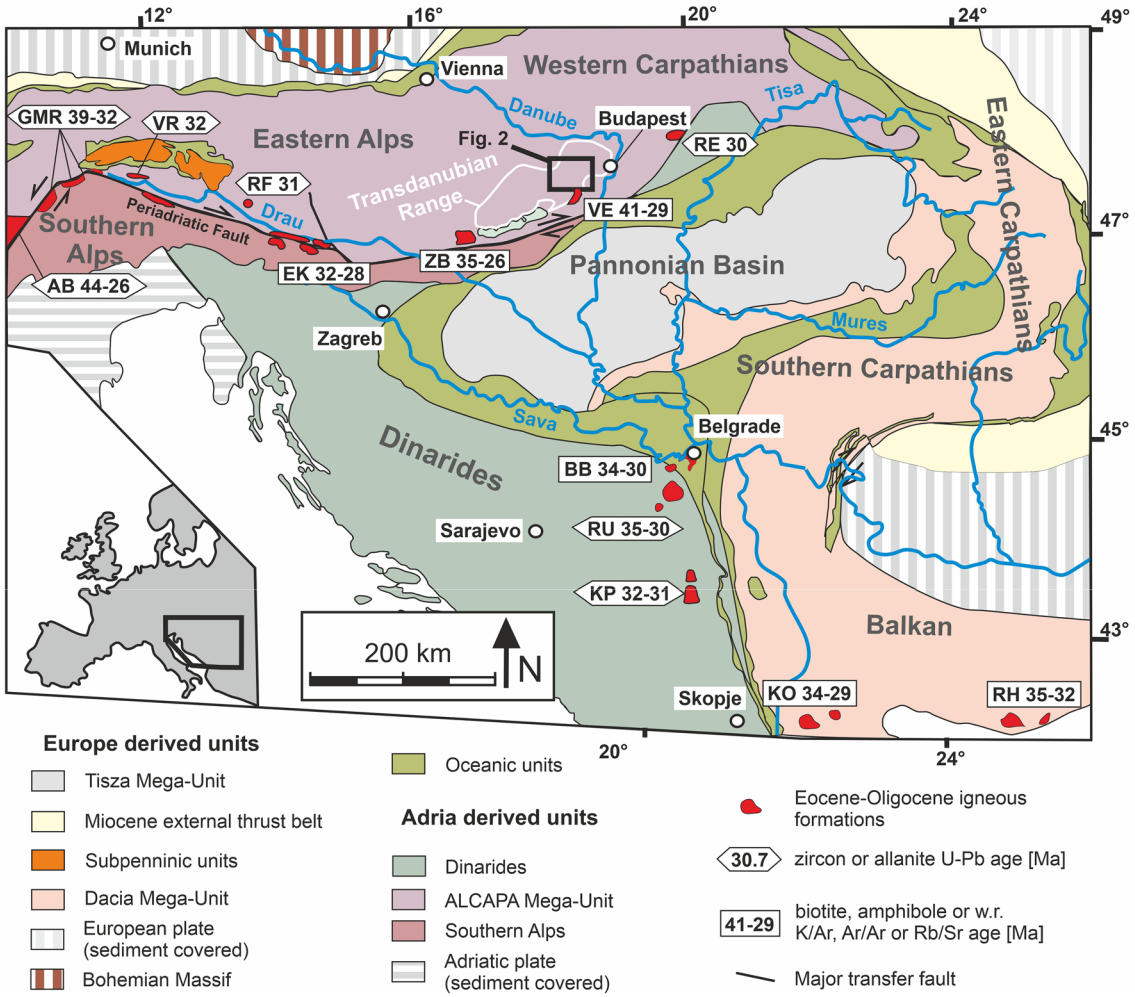

Fig. 1 Regional geological sketch map including the major occurrences of zircon-bearing Eocene–Oligocene intrusions and volcanic complexes and their ages. AB = Bergell and Adamello (Villa and von Blanckenburg 1991; Rosenberg 2004; Schaltegger et al. 2009; Skopelitis et al. 2011; Bergomi et al. 2015; Samperton et al. 2015; Ji et al. 2013, 2019; Tiepolo et al. 2014), BB = Boranja (Pamić and Balen 2001), EK = Eisenkappel (Scharbert 1975, Fodor 2008), GMR = Giudicaria Meran-Mauls and Rensen (Barth et al. 1989; Pomella et al. 2011), KO = Kratovo-Osogovo (Boev and Yanev 2001), KP = Kopaonik (Schefer et al. 2011), RE = Recsk (Arató et al. 2018), RF = Reifnitz (Neubauer et al. 2018), RH = Rhodope (Marchev et al. 2004), RU = Rudnik Mts. (Cvetković et al. 2016), VE = Velence Hills (Gyalog and Horváth 2004), VR = Vedrette di Ries (Romer and Siegfried Siegesmund, 2003), ZB = Zala Basin (Benedek 2002; Benedek et al. 2004). Base map is after Schefer et al. (2011). Black box indicates the position of the study area within the Transdanubian Range

rocks of the TR, due to their tectonic position, were exposed to terrestrial weathering and denudation several times (Kaiser 1997; Csillag and Sebe 2015). The reoccurring subaerial exposure periods resulted in the widespread formation of diverse weathering products, mainly not only bauxites, but also red clays and kaolinitic clays (Taeger 1909; Nemecz and Varju 1967; Kaiser 1997; Budai et al. 2008; Bárdossy 2013). *Oxisols*, the equivalents of bauxites in soil science, typically require at least 1 Ma to develop (Birkeland 1984, Retallack 1990). Although, the actual time of development is strongly controlled by geomorphological and climatic parameters. The termination of the deposition of these bauxitic rest sediments is mostly inferred from the ages of the overlying strata. However, the precise stratigraphic position of the typically fluvial or lacustrine cover sequences is often poorly constrained. The existence of detrital zircon grains in the bauxitic deposits has been known for a long time (e.g., Kiss 1955; Vörös 1958; Mindszenty et al. 1991; Boni et al. 2012). Paleogene fission-track ages of euhedral zircons from bauxite deposits (Dunkl 1992) demonstrated the potential to date the sediment sources, but with significant uncertainty in the single-grain ages (~ 3.5–5 Myr). Detrital zircon U–Pb geochronology offers considerably better precision than fission-track dating and has been successfully applied to karst-filling ferallitic sediments (~ 0.5 Myr uncertainty for Miocene ages in Kelemen et al. 2021).

Here we apply detrital zircon U–Pb geochronology and heavy mineral analysis to Paleogene bauxite deposits and the overlying cover formations of the Vértes Hills (VH), located at the northeastern side of the TR. The aim of the study was to identify potential source formations and constrain the depositional age of individual bauxite occurrences and their stratigraphic relations. Our results suggest that most of these sedimentary units contain redeposited zircons, which help to infer the Palaeozoic to Mesozoic source rocks exposed at the time of deposition, including paleogeographic implications. On the other hand, all deposits contain volcanic zircon crystals directly supplied by the contemporaneous Paleogene volcanic edifices of the Alps (Fig. 1). The youngest age components of these airborne contributions determine a maximum age of deposition of both the bauxitic deposits and the so far undated sandstones of the fluvial cover sequences. The zircon U–Pb age distributions could also reveal potential resedimentation relationships between the studied bauxitic deposits and their cover.

Geological setting

Since Late Palaeozoic times, the TR and the VH were part of the Neotethys rifted margin, situated between the former positions of the Northern Calcareous Alps and the Southern Alps (Kázmér and Kovács 1985; Haas et al. 1995; Héja et al. 2018). The TR became part of the uppermost Eastern Alpine nappes during the late Early to Late Cretaceous. As a topographically and structurally high unit, the TR underwent modest Paleogene deformation related to subduction below the Alps and Carpathians during the Eocene and Oligocene tectonic phases (Tari et al. 1993; Kázmér et al. 2003). From the latest Oligocene, the TR became detached from the Alpine realm along the Periadriatic Fault (Fig. 1.), juxtaposed other tectonic blocks and finally formed a part of the pre-rift basement of the Miocene Pannonian Basin (Kázmér and Kovács 1985; Csontos et al. 1992; Balázs et al. 2016; Tari et al 2021).

The basement of the TR is composed of Variscan low-grade metamorphic rocks including granitoid bodies covered by Permian clastic deposits and lagoonal evaporites (Budai et al. 1999). The main mass of the TR is composed of 2–3 km-thick Middle to Upper Triassic platform limestone and dolomite assemblage, overlying Lower Triassic mixed siliciclastic ramp sediments and lower Middle Triassic (Anisian) rift-related carbonates (Haas and Budai 1995; Rostási et al. 2011; Budai and Vörös 2006; Fig. 2). Anisian-Ladinian zircon-rich bentonites and volcaniclastics are often referred to as "pietra verde" (Szabó and Ravasz 1970; Budai and Vörös 2006; Kázmér and Kovács 1985; Mundil et al. 1996; Pálfy et al. 2003). However, ongoing volcanic activity is documented also for Carnian formations; subvolcanic andesite dikes occasionally crosscut the Triassic suite probably have less relevance in terms of sediment provenance due to their lower zircon content and restricted areal distribution (Haas et al. 2017; Dunkl et al. 2019). During the Jurassic and Early Cretaceous, the former Mesozoic carbonate platforms became submerged, dismembered and a horst-and-graben style submarine paleotopography has developed (Vörös and Galácz 1998).

The post-Barremian tectonic evolution of the TR is characterized by several folding and thrusting phases, which resulted in an alternation of subaerial denudation and marine sedimentation periods (Haas 1991; Fodor 2008; Tari and Horváth 2010; Csillag and Sebe 2015). Two distinct terrestrial to marine sedimentary cycles developed (Fig. 2b) from middle Albian to Cenomanian (Császár 1986; Góczán et al. 2002) and Santonian to Campanian (Haas 1983). These cycles sealed the folded structures with occasional Cretaceous bauxite deposits at their base (Fig. 2, Albian and Santonian bauxites).

The early Paleogene is marked by moderate tectonic activity in the TR, the ongoing minor shortening generated uplift, which resulted in a subsequent period of subaerial exposure of the entire TR from latest Cretaceous to Lutetian. As a combination of the folding and denudation, enhanced by the tropical warm-humid climate of the late Paleocene Thermal Maximum, the Jurassic and Cretaceous strata were significantly eroded and a karstic planation surface formed

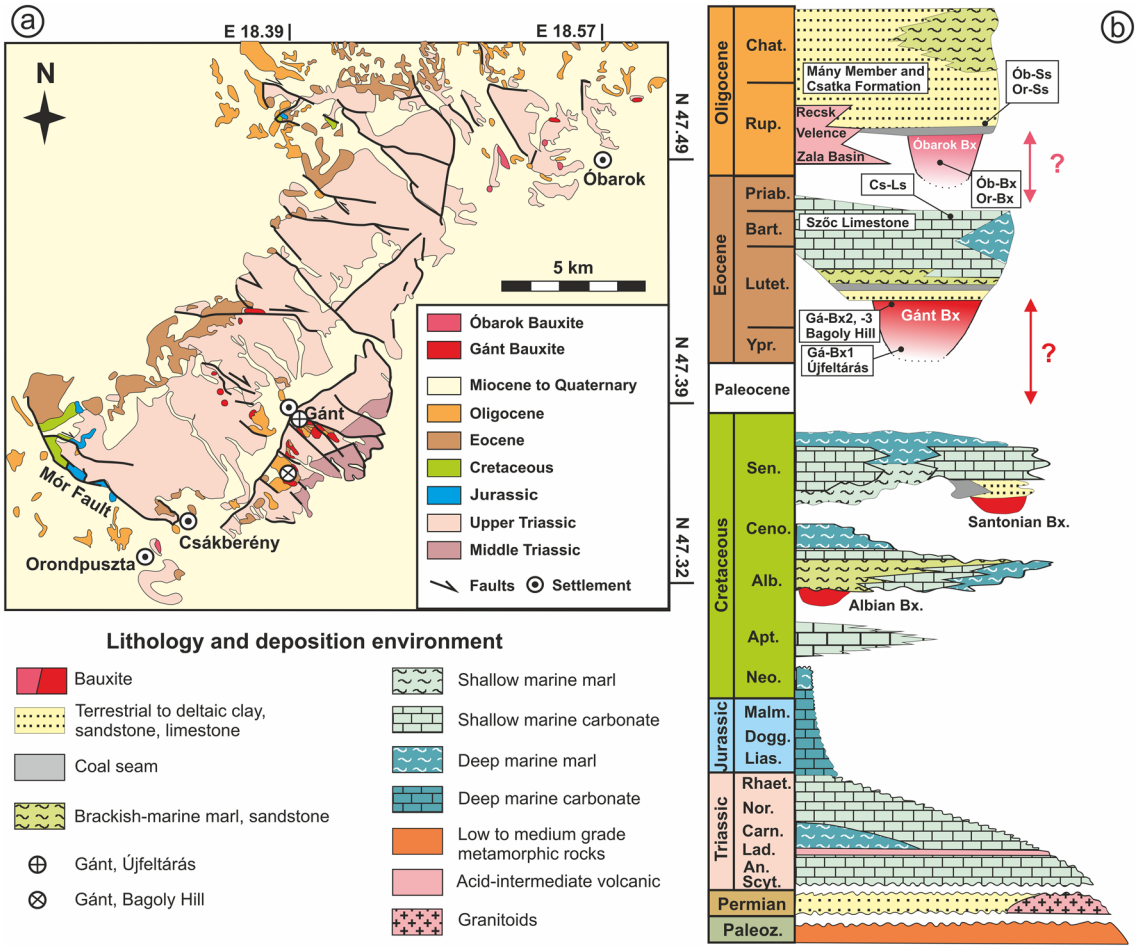

Fig. 2 Simplified geology of the Vértes Hills (**a**) and general stratigraphy of the Transdanubian Range and its forelands (**b**) (modified after Benedek et al. 2002; Gyalog 2005; Budai et al. 2008). Double-headed arrows with question marks represent the hitherto existing uncertainty in the formation age of the bauxite deposits within the hiatus

and culminated in karstification of the Triassic carbonates (Szantner and Szabó 1969; Dudich and Komlóssy 1969; Csillag and Sebe 2015). Furthermore, an extensive bauxitic blanket was developed, which generally covered the TR (Mindszenty et al. 2000). These deposits are described as Gánt Bauxite Formation (Fig. 2b) characterized by the alternation of pelitomorphic bauxite and bauxitic conglomerates with an average thickness of 20–25 m, at places reaching up to 60 m (Bernhardt 1990; Mindszenty 2000; Kercsmár et al. 2008; Kercsmár 2018). The semi-quantitative heavy mineral data of some Gánt Bauxite occurrences led Mindszenty et al. (1991) to suggest an Alpine provenance from metamorphic and igneous rocks exposed in the hinterland of the bauxite deposits at the time of their sedimentation. The ages of the volcanogenic source rocks were determined by detrital zircon fission-track dating as Ypresian to Lutetian (Dunkl et al. 1992). The Gánt Bauxite deposits became covered by transgressive sequences in two steps during the middle Eocene. First, as a result of rising groundwater table and dissected karst terrain, inland blue-holes formed with sedimentary sequences indicating gradually increasing salinity from freshwater to brackish to schizohaline, followed by the marine transgression of the nummulitic Szőc Limestone, which covers the majority of the TR (Fig. 2b; Bignot et al. 1985; Kázmér et al. 2003; Carannante et al. 2004; Pálfalvi 2007; Kercsmár et al. 2008; Bárdossy 2010; Mindszenty 2010; Trabelsi et al. 2021).

The latest Eocene uplift of the VE caused partial erosion of the Cretaceous to Eocene strata; the denudation locally excavated the Eocene sediments, including bauxite deposits and reached even their Mesozoic substratum. Telegdi-Roth (1927) identified this event as early Oligocene erosion and referred to it as 'infra-Oligocene denudation', which eroded most of the regressive sedimentary units of the deep marine Eocene basins of the TR (Báldi 1986). The Oligocene Óbarok Bauxite (Fig. 2b) is thought to represent this denudation period; it is also considered to be partly redeposited from the former Gánt Bauxite

deposits (Mindszenty 1969; Böröczky 1996; Selmeczi 2008). The age of these weathering products was indirectly constrained by the overlying fluvial to marine clastics as Oligocene based on molluscs, plant remnants and an iron-mineralized (hematitic) tree trunk (Báldi 1986; Mindszenty et al. 2002; Hably et al. 2015). Since early Oligocene times, as a result of intense uplift and erosion in the Alpine region, and concomitant subsidence in adjoining terranes, large parts of the TR were covered with the up to 800 m-thick siliciclastic assemblage of the Csatka Formation, deposited by a paleo-river system identified as the precursor of the modern Drau River (Fig. 1; Korpás 1981; Benedek et al. 2001; Danišík et al. 2015). The river system supplied sediment into a co-existing brackish to marine basin which resulted in the deposition of the siliciclastic Mány Member (Fig. 2b; Báldi-Beke and Báldi 1985; Selmeczi 2008).

This Eocene to Oligocene sedimentation in the TR was coeval with the Paleogene igneous activity of the Alpine-Carpathian-Dinaric region lasting mostly from 44 to 26 Ma (Fig. 1). In the Pannonian Basin, the stratovolcanic edifices are well preserved in the Zala Basin, Velence Hills and Recsk (Figs. 1, 2b); however, the volcanic complexes in the Alps are deeply eroded and thus, only, the intrusive roots are preserved. The traces of igneous activity are present in the peri-Alpine, intra-Carpathian and Dinarid basins in the form of ash layers, volcanoclastic layers, volcanic pebbles, diagnostic heavy mineral assemblages in siliciclastic sedimentary rocks and the characteristic zircon U–Pb or mica K–Ar ages (e.g., Brügel et al. 2000; Benedek et al. 2001; Lu et al. 2018; Di Capua et al. 2021).

Materials

Altogether eight bulk rock samples were processed for heavy mineral analysis and U–Pb zircon dating each with a starting dry mass of ca. 1.5–3.5 kg. The locations and lithologies are summarized in Table 1. Photo documentation of the outcrops and samples are available in Supplementary Data S1.

The Gánt bauxite

At the formerly excavated and well-exposed Gánt bauxite deposit sedimentological data suggest that a primarily developed bauxitic blanket underwent massive erosion and large-scale resedimentation in a soft-sediment deformation style caused by synsedimentary tectonic events (Mindszenty et al. 1989; Mindszenty 2010). Samples were collected to serve as representatives of the Eocene-covered bauxites of the VH. Sample Gá-Bx1 is a light grey, pelitomorphic bauxite collected from the base of the Újfeltárás deposit, close to the underlying Upper Triassic carbonate (Fig. 2b). Gá-Bx2 is red pelitomorphic bauxite from the top of the Bagoly Hill deposit, close to the middle Eocene cover sequence, while sample Gá-Bx3 is a yellow–red bauxite conglomerate with up to 2 cm bauxitic pebbles (Fig. 2b).

The immediate freshwater limestone cover, which is overlain by brackish to schizohaline sediments intercalated with lignitiferous layers, contains Charophyte species ranging from lower Lutetian to upper Bartonian (Trabelsi et al. 2021). The upsection following marly cover of the Gánt bauxite deposit (Fig. 2b) did not contain sufficient amounts of diagnostic or datable heavy minerals.

Table 1 Sample locations and brief description

Code	Location	Latitude	Longitude	Nomenclature	Lithology	Remarks
Ób-Ss	Óbarok, NE Vértes Hills	N47.50111	E18.57750	Mány Member	Yellow fine to medium grained sandstone	Immediate cover of bauxite
Ób-Bx	Óbarok, NE Vértes Hills	N47.50083	E18.57416	Óbarok Bauxite	Light red bauxite	Close to bedrock
Or-Ss	Orondpuszta, SW Vértes Hills	N47.33555	E18.30368	Csatka Formation	Light grey sandstone	Cover of the bauxite above some 10 cm coal seams (Fig. S1)
Or-Bx	Orondpuszta, SW Vértes Hills	N47.33555	E18.30368	Óbarok Bauxite	Yellow/red bauxite	Multi layer
Cs-Ls	Csákberény, SE Vértes Hills	N47.35083	E18.32722	Szőc Limestone	White limestone	Multi layer
Gá-Bx3	Bagoly Hill, Gánt, S Vértes Hills	N47.36653	E18.38300	Gánt Bauxite	Yellow/red bauxite with < 2 cm bx. pebbles	Close to cover
Gá-Bx2	Bagoly Hill, Gánt, S Vértes Hills	N47.36653	E18.38300	Gánt Bauxite	Red pelitomorphic bauxite	Close to cover
Gá-Bx1	Újfeltárás, Gánt, S Vértes Hills	N47.38490	E18.39740	Gánt Bauxite	Grey bauxite	Close to bedrock

The nomenclature is based on Budai and Fodor (2008)

The Szőc limestone

The shallow marine Szőc Limestone generally belongs to the NP16 nannozone (late Lutetian to early Bartonian; Nagymarosy and Báldi-Beke 1988; Báldi-Beke 2003; Kollányi et al. 2003; Ozsvárt 2003). The studied Szőc Limestone karst infill sample represents the topmost part of the Gánt Bauxite cover sequence, which was dated as uppermost Bartonian to earliest Priabonian through Nummulites and nannoplankton studies (Báldi-Beke 1984; Bernhard 1990; Pálfalvi 2007; Kercsmár et al. 2008). A late Eocene subaerial exposure of the Szőc Limestone is suggested by a 25-m siliciclastic intercalation overlain by a new series of late Eocene carbonatic sequences found in the nearby Lb-II borehole (Kercsmár et al. 2008).

We collected samples at Csákberény from the uppermost part of the Szőc Limestone Formation (Cs-Ls) that represent the cover sequences of the Gánt Bauxite (Fig. 2). The material is loose calcareous sand dominated by the fragmented local limestone with barely visible siliciclastic contribution, trapped at the bottom of a collapsed karstic cavity.

The Óbarok bauxite

The Óbarok Bauxite is generally described as the Oligocene-covered bauxite level in the TR (Selmeczi 2008). Bauxites along with their immediately overlying siliciclastic sediments of the Mány Member were sampled at the type locality in the Óbarok open-pit (Ób-bx) located at the northern part of the Vértes Hills (Fig. 2a). The bauxite is red, pelitomorphic and the sample represents the low-grade, argillaceous base of the deposit, close to the underlying Triassic carbonate. The immediate cover of the bauxite is a yellow, medium- to coarse-grained sand of the Mány Member (Ób-Ss). At the Óbarok site, the age of bauxite deposition was roughly estimated by a hematitized trunk of a tree species existing since the Oligocene that was found in the uppermost 2 m of the bauxite deposit (Mindszenty et al. 2002).

The southern occurrence of the Óbarok Bauxite in the VH is represented by yellow and red, pelitomorphic bauxites collected in the Orondpuszta open-pit (Or-Bx). This bauxite locality forms shallow sinkholes with a maximum depth of 5 m (Fig. 2a). The age of the bauxite at this location was estimated as Oligocene by the gastropod fauna found in the immediate cover of several 10 cm-thick coal seams (Selmeczi 2008). The Csatka Formation, overlying the coal seams, was sampled via a micaceous, siliciclastic, grey sandstone (Or-Ss) that accumulated in outcrop-sized half grabens reflecting synsedimentary fault activity. The maximum thickness of the sand exceeds 100 m (Supplementary Data S1; Fodor 2008). Neither geochronological data nor heavy mineral-based provenance information was hitherto available from the Óbarok Bauxite.

Methods

The mineralogical composition of the whole rock samples was determined by X-ray powder diffraction analysis (XRD) at the Eötvös Loránd University of Budapest, Hungary and the Geoscience Center of Göttingen University, Germany. Bauxite samples of 500–2000 g have been crushed and sieved to 63–125 µm for optical heavy mineral analysis and LA-ICP-MS zircon U–Pb geochronology. After 5% acetic acid treatment, the boehmitic-hematitic aggregates have been disintegrated by a high-energy ultrasonic homogenizer, which leaves the detrital heavy mineral grains intact. Heavy mineral separation has been performed by using 2.89–2.93 g/cm^3 Na-polytungstate solution. Whenever it was possible, optical heavy mineral identification was done using the Ribbon counting method or randomly on ~ 200 detrital transparent and translucent, non-micaceous grains per sample embedded in Meltmount immersion medium of $n = 1.66$ refractive index as proposed by Mange and Mauer (1992).

Zircon grains for U–Pb dating were randomly selected and embedded into epoxy mounts. In-situ U–Pb dating was carried out at the GÖochron Laboratories of the Geoscience Center Göttingen, using a Resonetics excimer laser ablation system coupled to an Element2 sector field ICP-MS following the techniques described by Frei and Gerdes (2009). Further details about the U–Pb analytical technique can be found in Kelemen et al. (2017) and Sliwinski et al. (2017). The precision and accuracy of the zircon U–Pb ages can be estimated by the compilation of 121 measurements performed on 16 age reference materials (secondary standards; see Supplementary Data S2). The age components were identified and Kernel Density Estimation plots were generated by the DensityPlotter software (Vermeesch 2012).

Results

X-ray powder diffraction data

Table 2 summarizes semiquantitative proportions of the mineral phases of the samples. The corresponding XRD diffractograms are presented in Supplementary Data S3. The bauxites from Gánt have mainly boehmitic and kaolinitic compositions. Ti-carrying phases appear as anatase in the Bagoly Hill samples (Gá-Bx3, Gá-Bx2). Chlorite was detectable at both the Újfeltárás and Bagoly Hill locations. The Újfeltárás bauxite (Gá-Bx1) contains gypsum, while traces of dolomite are present in sample Gá-Bx2.

The bauxites from the Óbarok and Orondpuszta locations contain kaolinite and hematite alike; however, strong

Table 2 Mineralogy of whole-rock samples, according to XRD analyses

Code	Gá-Bx1	Gá-Bx2	Gá-Bx3	Ób-Bx	Ób-Ss	Or-Bx	Or-Ss	Cs-Ls
Sample	Grey pel. bauxite	Red pel. bauxite	Pebbly bauxite	Bauxite	Sandstone	Bauxite	Sandstone	Limestone
Location	Újfeltárás, Gánt	Bagoly H., Gánt	Bagoly H., Gánt	Óbarok	Óbarok	Orondpuszta	Orondpuszta	Csákberény
Calcite					+		++	+++
Dolomite		+			+++		++	
Quartz					+		+++	
Gypsum	++							
Muscovite				(+)	+		+	
Chlorite	+	+	+			(+)	+	
Kaolinite	+++	+++	+	+++	++	++		
Boehmite	+++	+++	+++					
Gibbsite						+++		
Hematite				+		+		
Goethite				++	+			
Rutile	+							
Anatase	+	+	+			++		
Brookite				+				

Evaluated diffractograms are attached in Supplementary Data S3

+++ Most intense peaks

++Moderately intense peaks

+Detectable phases

and characteristic gibbsite peaks were acquired from the bauxite collected at Orondpuszta. The main iron-bearing phase at Orondpuszta is hematite, while at Óbarok goethite is more dominant. The two bauxite samples show differences in TiO_2 phases. While the bauxite from Óbarok contains brookite, the Orondpuszta bauxite contains anatase. The covering siliciclastic sequences of the Mány Member and Csatka Formation (Fig. 2b) are dominated by dolomite, quartz and kaolinite, while calcite, muscovite and goethite were also detected in their samples.

Heavy mineral spectra

The detailed data are presented in Supplementary Data S4. Sample Gá-Bx1 from Újfeltárás shows a high amount of authigenic grains (composites of µm-sized particles, mainly Al–Fe–Ti oxides-hydroxides). The majority of the translucent detrital heavy minerals is zircon, which is mostly euhedral (~68% of zircon crystals). Besides zircon, the Gá-Bx1 sample also revealed garnet, TiO_2-minerals, epidote-group minerals and xenotime-monazite grains. Minor amounts of tourmaline and sphene were also identified (Fig. 4). Sample Gá-Bx3 from Bagoly Hill contains euhedral ilmenite crystals and their brownish pseudomorphs, while the translucent detrital heavy minerals are dominated by zircons which are mostly euhedral (~76% of zircon crystals, Figs. 3 and 4). Besides zircon, garnet is present as well along with minor amount of TiO_2-minerals, tourmaline, epidote-group minerals, pyroxene and apatite (Fig. 4).

The heavy mineral suite of the arenaceous sample of Szőc Limestone (Cs-Ls) is mostly composed of non-altered opaque minerals. Euhedral ilmenite and magnetite crystals are frequently observed (Fig. 3). The detrital, translucent, non-micaceous heavy mineral grains are dominated by garnet and zircon (~77% of them are euhedral). Significant amounts of epidote-group minerals have been revealed, as well and minor amounts of TiO_2-minerals, tourmaline, sphene and staurolite (Fig. 4).

The heavy mineral suite of the Orondpuszta bauxite (Or-Bx) is mostly composed of zircons (72% are euhedral). TiO_2-minerals, tourmaline, kyanite, staurolite, pyroxene and amphibole grains are present in minor amounts as well (Fig. 4). The heavy mineral suite of the cover sand at Orondpuszta (Or-Ss) is mostly composed of garnets and epidote-group minerals. Besides, zircons (29% euhedral), staurolite, pyroxenes, TiO_2-minerals, tourmaline, sphene, kyanite and sillimanite have been detected (Fig. 4).

The heavy mineral suite of the Óbarok bauxite (Ób-Bx) is dominated by zircons (~71% euhedral). Garnet, epidote-group minerals, TiO_2-minerals, staurolite and tourmaline are present, too (Fig. 4). The heavy mineral suite of the cover sand (Ób-Ss) contains a high amount of sometimes euhedral but mostly irregular or strongly transformed opaque crystals, while the translucent spectrum is again dominated by zircons (71% euhedral; Fig. 3) and TiO_2-minerals.

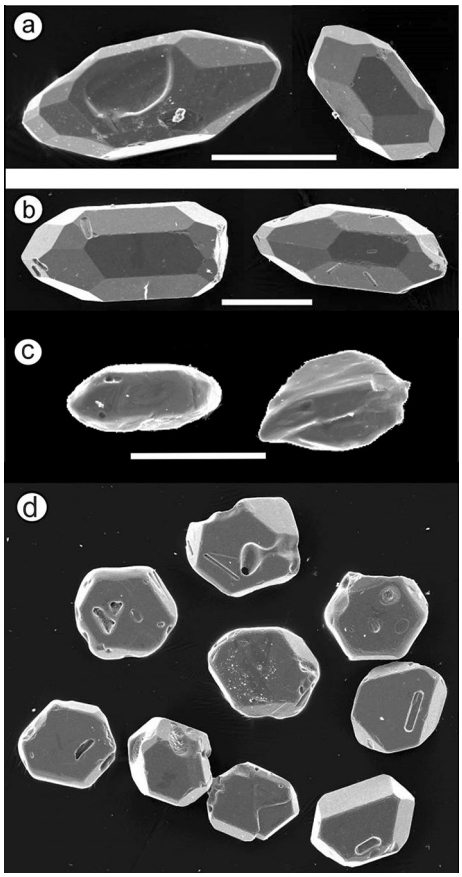

Fig. 3 Scanning electron microscopic images of euhedral zircon crystals from the Gánt Bauxite (**a**) and from the Óbarok sandstone (**b**). White bars represent 100 µm. Remarkable that the bauxite-hosted crystals do not show chemical corrosion features, the crystal edges and faces are fully preserved. Reworked zircon crystals with abraded edges from the Orondpuszta bauxite (**c**). **d** Scanning electron microscopic image of some characteristic, euhedral and slightly resorbed ilmenite crystals from the Szőc Limestone (Cs-Ls). Similar crystals occur actually in all samples where the Paleogene zircons are present and are especially abundant in the Óbarok cover sandstone (Ób-Ss). The diameter of the crystals is ca. 150 µm

Zircon U–Pb ages

The raw U–Pb data are documented in Supplementary Data S5. Out of 729 total single grain shots, 636 are concordant between 90 and 110%; these single-grain ages were used for further evaluations and interpretations. The 245 concordant ages from the Gánt Bauxite Formation contain a relatively high proportion of Paleogene ages (29% to 65%) in a relatively narrow range of 45.7 ± 1.0 to 40.7 ± 1.1 Ma (Fig. 5). Besides these Paleogene ages, Archean to older Neoproterozoic (> 700 Ma), Late Neoproterozoic to Cambrian and Devonian to Carboniferous ages are also present. A remarkable feature of all three Gánt Bauxite samples is the relatively high proportion (~ 13% to 30%) of Middle to early Late Triassic zircons (Fig. 5). The dissolution residue of the Szőc Limestone from Csákberény (Cs-Ls) contains almost exclusively Paleogene zircon crystals, 42 out of the total 43 concordant ages, with a tight distribution between 41.5 ± 0.6 and 36.4 ± 1.1 Ma. The Orondpuszta bauxite (Or-Bx) and the overlying sandstone (Or-Ss) reveals also Paleogene ages (~ 97 and 93%; Fig. 5). Paleogene ages dominate the Óbarok bauxite sample (Ób-Bx) as well, with values ranging from 41.6 ± 0.9 to 30.9 ± 0.7 Ma. However, the cover sand of the Óbarok bauxite (Ób-Ss) contains some Archean to older Neoproterozoic and Late Neoproterozoic to Carboniferous zircon ages, similar to the pre-Cenozoic age components of the Gánt Bauxite samples except for the complete lack of Anisian–Carnian ages (Fig. 5).

The age distributions obtained in the samples were compared by the Kolmogorov–Smirnov test (Press et al. 1986; Guynn and Gehrels 2010). The test was performed both on the entire age range and on the Paleogene ages only (Fig. 6). A part of the Gánt bauxite shows similarities and also the youngest Ób and Or samples yield *P* values above 0.05, which level is considered as the threshold for similarity. Remarkably none of the sample pairs that were deposited below and above the Szőc Limestone show similarities with a probability higher than 0.1%.

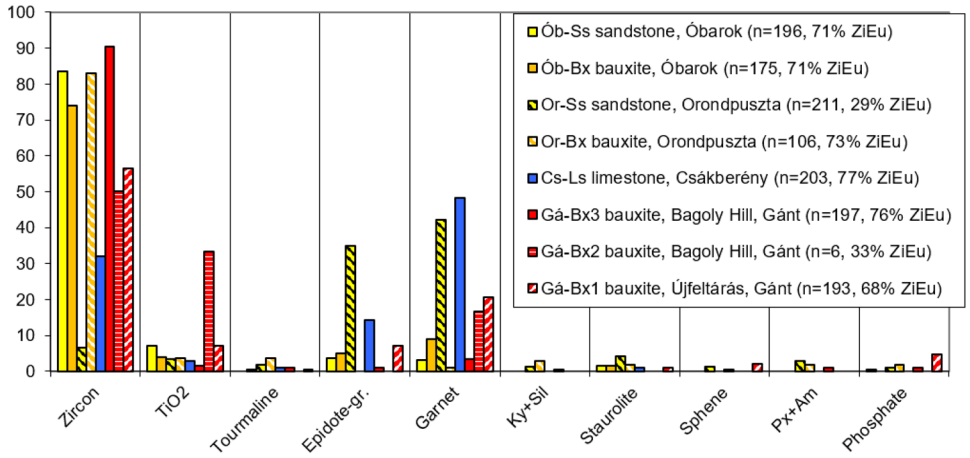

Fig. 4 Translucent heavy mineral data of the analysed samples (TiO_2 = rutile + anatase + brookite, Ky = kyanite, Sil = sillimanite, Px = pyroxene, Am = amphibole, Phosphate = apatite + monazite + xenotime). Numbers in brackets indicate total heavy mineral grains analysed and the percentage of euhedral zircons compared to the total number of zircons (e.g., 71% ZiEu). Further details are provided in Supplementary Data S4

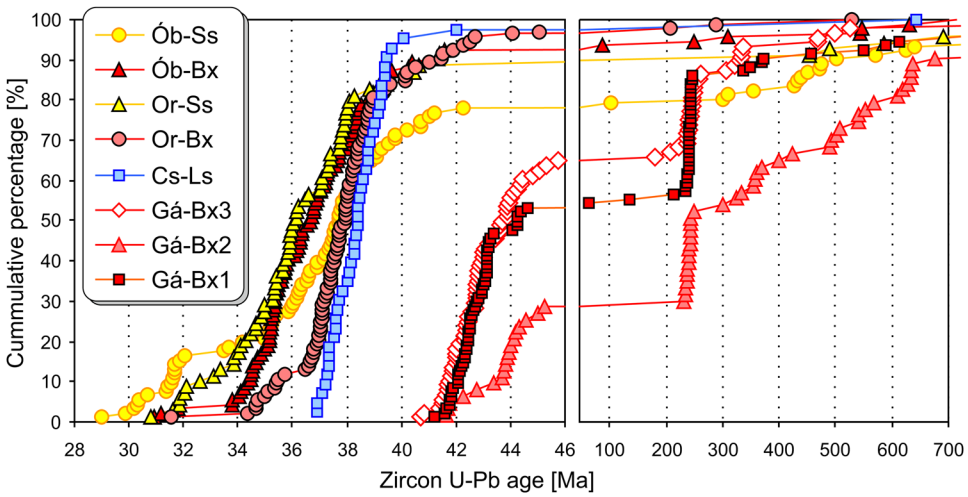

Fig. 5 Cumulative plot of the considered 636 U–Pb ages (90–110% concordance) obtained on the bauxite and cover sediment samples from the Vértes Hills, Hungary (Bx: bauxite, Ls: limestone, Ss: sandstone, more details in Table 1). The ages older than 700 Ma are not shown, their provenance significance is subordinate (see all raw U–Pb data in Supplementary Data S5). Please note the cut at 46 to 60 Ma along with a change in scale

Only Paleogene ages (50 to 29 Ma) / All U-Pb ages considered	Ób-Ss	Ób-Bx	Or-Ss	Or-Bx	Cs-Ls	Gá-Bx1	Gá-Bx2	Gá-Bx3
Ób-Ss		0.316	0.605	0.025	0.001	0.000	0.000	0.000
Ób-Bx	0.210		0.897	0.002	0.000	0.000	0.000	0.000
Or-Ss	0.643	0.999		0.000	0.000	0.000	0.000	0.000
Or-Bx	0.059	1.000	0.892		0.426	0.000	0.000	0.000
Cs-Ls	0.175	1.000	0.969	1.000		0.000	0.000	0.000
Gá-Bx1	0.000	0.000	0.000	0.000	0.000		0.629	0.363
Gá-Bx2	0.000	0.000	0.000	0.000	0.000	0.000		1.000
Gá-Bx3	0.000	0.000	0.000	0.000	0.000	0.000	0.566	

Fig. 6 Results of Kolmogorov–Smirnov test for the detrital zircon U–Pb age distributions of the Vértes Hill samples. The table includes probability (P) values calculated by the "K-S Test" Excel macro (Guynn and Gehrels 2010). Grey fields indicate P values > 0.05 implying that the respective zircon age distributions are not significantly different. The line separates the K-S tests performed on the entire range of obtained ages (lower triangle) and on the Paleogene ages only (upper triangle)

The age component analysis presents a highly consistent pattern, which shows strong similarity for all Gánt Bauxite samples (Fig. 7). This similarity is further enhanced by the general presence of the Anisian–Carnian and Variscan age components (Table 3). The fairly distinctive 38.3 Ma component of the karst infill in the Szőc Limestone seems to appear consequently with similar age components (37.4–38.4 Ma) in all of the Óbarok and Orondpuszta samples, bauxites and sandstones alike, while the Pre-Cenozoic age components are either underrepresented (Ób-Ss) or missing (Fig. 5; Table 3). Moreover, three out of four Óbarok and Orondpuszta samples share similar younger age components at 35.1–35.5 Ma and 31.2–32.4 Ma, respectively (Table 3).

To summarize, the U–Pb age components of the Gánt bauxites are markedly different from the Orondpuszta and Óbarok bauxites. The Cenozoic zircons from Gánt are restricted to the late Lutetian, while such ages are subordinate at Orondpuszta and Óbarok. In contrast, the latter localities show distinct Bartonian to Rupelian age components. A further striking difference is the high percentage of Pre-Cenozoic ages in the Gánt bauxites, which have only a minor share or are completely missing in the two other bauxite deposits (Table 3).

Discussion

Major sources of the bauxites and their cover sequences

The heavy mineral composition and the detrital zircon age spectra allow for identifying well distinguishable sources of the bauxite and the cover deposits. We present the major sources according to their characteristic zircon U–Pb ages.

Coeval Paleogene felsic-intermediate volcanism

The Paleogene zircons form the youngest age components and these crystals carry the most important stratigraphic information. The dominantly euhedral zircons together with the presumably co-genetic amphibole, pyroxene and euhedral ilmenite grains derive from the Alpine, Pannonian or

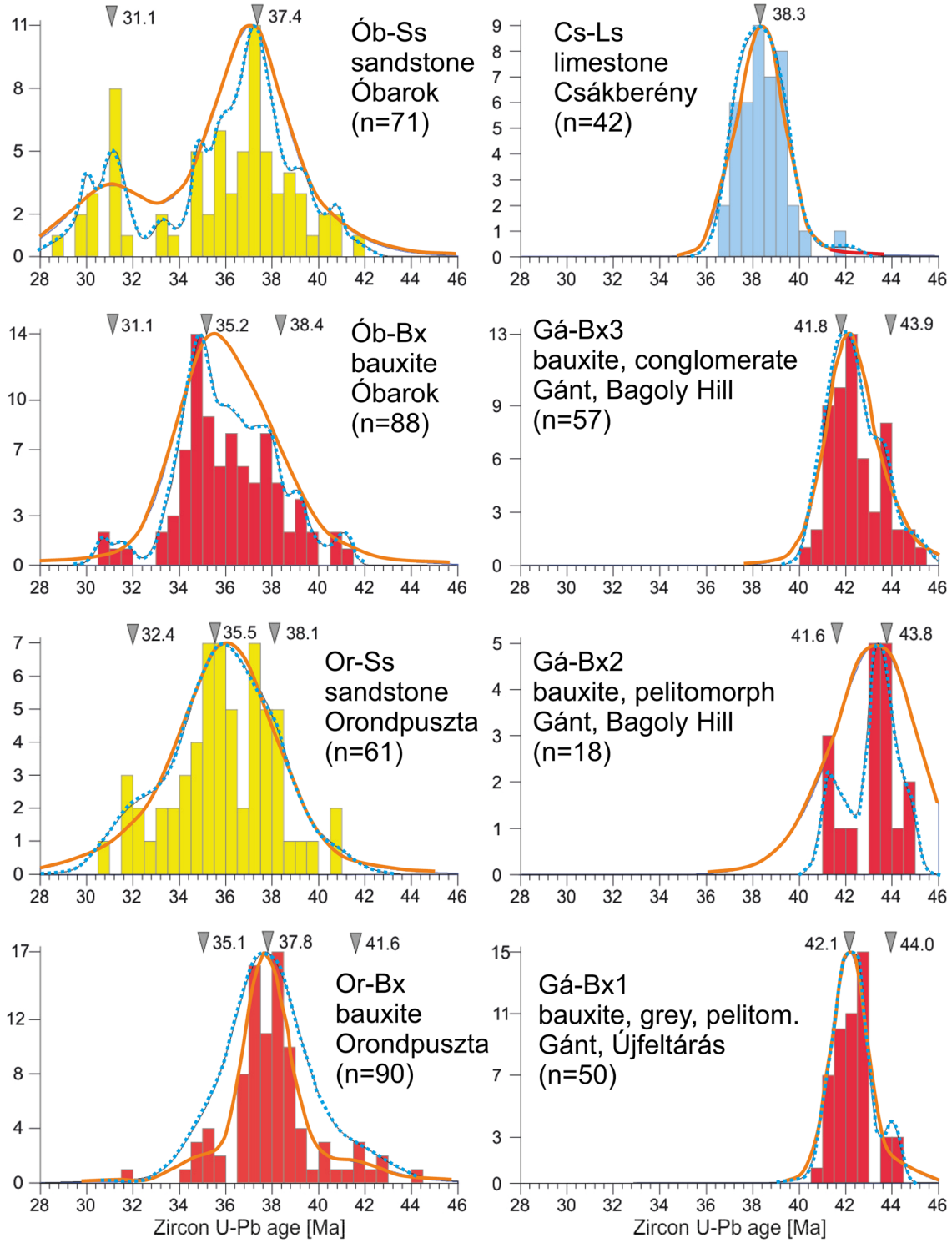

Fig. 7 Age spectra and age components of the Paleogene detrital zircon U–Pb ages obtained in the bauxite horizons and their cover formations. The components—represented by triangles—are identified by DensityPlotter software (Vermeesch 2012). The continuous curve represents kernel density estimation (bandwidth determined automatically) and the dashed curve represents probability density distribution (PDP; bin width of the bar plot is 0.5 Myr)

Table 3 Age components of the detrital zircon U–Pb data identified by the DensityPlotter software (Vermeesch 2012)

	Cenozoic age components [Ma]					Pre-Cenozoic age components [Ma]					
	Ol_Ru	Eo_Pr	Eo_Pr-Ba	Eo_Lu	Eo_Lu	T2	Var	Ord	N-Prot	P-Prot	N-Arch
Ób-Ss	31.1		37.4								
Ób-Bx	31.1	35.2	38.4								
Or-Ss	32.4	35.5	38.1								
Or-Bx		35.1	37.8	41.6							
Cs-Ls			38.3								
Gá-Bx3				41.8	43.9	238	354				
Gá-Bx2				41.6	43.8	238	357		520		
Gá-Bx1				42.1	44.0	242	326	487			
All samples	30.8	35.1	37.9	41.8	43.8	238	336	465	605	2016	2586

Ol_Ru Oligocene, Rupelian, *Eo_Pr* Eocene, Priabonian, *Eo_Pr-Ba* Eocene, Priabonian-Bartonian, *Eo_Lu* Eocene, Lutetian, *T2* Middle Triassic, *Var* Variscan, *N-Prot* Neoproterozoic, *P-Prot* Paleoproterozoic, *N-Arch* Neoarchean

Dinarid Paleogene volcanic complexes (Fig. 1), most likely by aeolian transport. Using the component identification method of Vermeesch (2012) five major Cenozoic eruption events can be documented in the studied formations, ranging from Lutetian to Rupelian times (~44 to ~31 Ma; Table 3). Figure 8 shows the comparison of the five age components identified in the Paleogene data from the VH to the major activity intervals of the zircon-dated volcanic complexes of the region. The latter is derived from the zircon data obtained from the Paleogene peri-Alpine basin deposits (i.e., Como Conglomerate, early Glarus, Ponte Pià Formation) as compiled by Lu et al. (2018). The ca. 44–41 Ma age range is underrepresented in the northern and southern peri-Alpine deposits, while they are well recorded in the VH bauxites and their covers. The source is identified exclusively as the Adamello complex (Fig. 1; Skopelitis et al. 2011; Ji et al. 2013; Tiepolo et al. 2014). The major, ca. 39–34 Ma age range corresponds to the source of the northern peri-Alpine deposits and is most probably also sourced by the Adamello complex, the most voluminous Paleogene igneous massif of the Alps (e.g., Pfiffner 2014). The amphibole, pyroxene and titanite crystals found in the bauxite and sandstone samples match well with the composition of the characteristic rocks of the Adamello complex and the subvolcanic dykes emplaced around it (Bergomi et al. 2015; Schaltegger et al. 2009). The 35-Ma age components might correspond to an

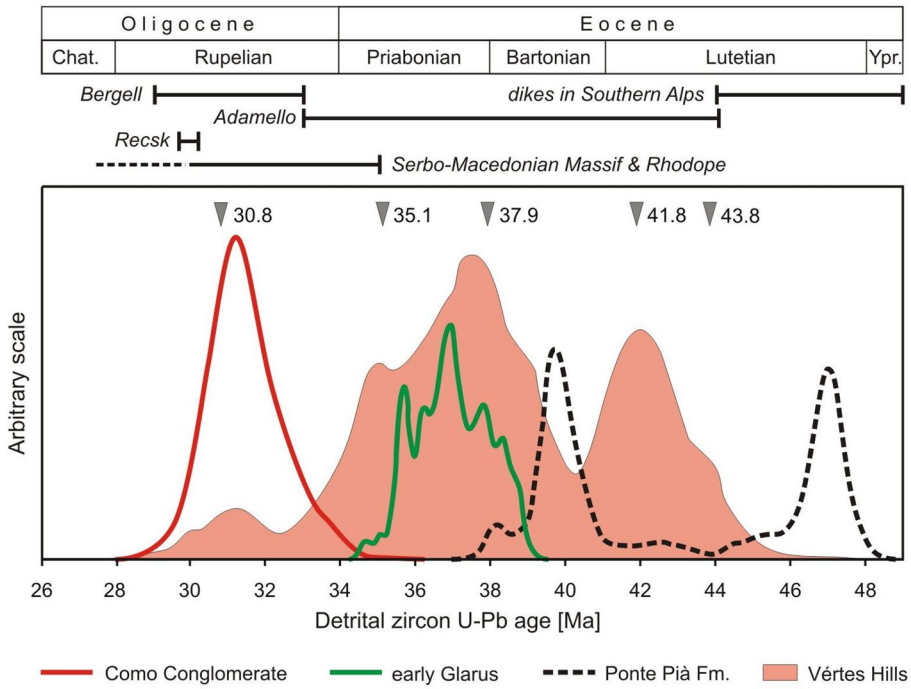

Fig. 8 Comparison of the Paleogene detrital zircon U–Pb ages from the Vértes Hills with detrital zircons from the peri-Alpine basin siliciclastic sequences (i. e., Como Conglomerate, early Glarus and Ponte Pià Formations; Lu et al. 2018). The shaded area represents all Paleogene U–Pb ages from the Vértes Hills; presented as probability density distribution in order to allow comparability to the published Alpine data. The grey triangles highlight the identified age components in the pooled Paleogene data from the Vértes Hills. The horizontal bars indicate the time intervals of major activity of the potential volcanic complexes, as dated by the zircon U–Pb method

initial volcanic phase in the Velence complex (Danišík et al. 2015). The youngest, small, but highly diagnostic age component (ca. 32–30 Ma) can derive from several sources. In this case, beyond the Alpine Bergell complex, some igneous centres in the Balkan peninsula or the Recsk and Velence complexes (situated within the Pannonian Basin) could be the source of these zircon crystals (Figs. 1 and 8).

Middle Triassic volcanic formations of the Transdanubian range

The Triassic zircon age components (242–238 Ma, Table 3) identified in the bauxite samples from the Gánt localities can be well associated with the Anisian–Lanidian volcanic formations that are widespread in the TR but also in the entire Southern Alpine–Dinaridic realm (e.g., Szabó and Ravasz 1970; Pálfy et al. 2003; Mundil et al. 1996; Olšavský 2001; Beltrán-Triviño et al. 2016; Haas et al. 2017; Kövér et al. 2018; Smirčić et al. 2018; Storck et al. 2019). Similar Triassic fission-track ages were already documented on detrital zircon crystals in the Gánt site deposits and some other Paleogene bauxite occurrences of the southern TR (Dunkl 1992). These zircons accumulated on the karstified surfaces and experienced only local transport towards the dolinas of the Gánt Bauxite deposits. A contribution of the dissolution residues of Triassic carbonates to the material of the bauxites in the TR has already been conceptually proposed by Komlóssy (1967).

The U–Pb age distributions in the Gánt Bauxite sample indicate perfect matching with the Anisian-Lanidian "pietra verde" tuff (Fig. 9). A few younger ages probably derive from Carnian igneous rocks. This distribution fits well with the abundance and zircon fertility of the two Triassic magmatic formations in the TR because the "pietra verde" is widespread in the intra-platform Triassic basins, and these tuff layers are rich in zircon crystals, while the younger, mostly intrusive andesitic formations have much smaller extent and they are relatively poor in zircons (Dunkl et al. 2019). Some of the euhedral ilmenite crystals might be assigned also to the Anisian-Lanidian tuffs.

Permian felsic formations

Figure 10 shows the comparison of the pre-Mesozoic zircon ages from the VH and the compilation of ages from the two most reliable source terranes. From the bauxites of the VH only six U–Pb data falls in the Permian period. The nearest and highly reliable sources of them could be the Permian felsic formations within the TR (Szemerédi et al. 2020) as in some areas of the TR the Palaeozoic formations were exposed to denudation in the Eocene (Kókay 1989).

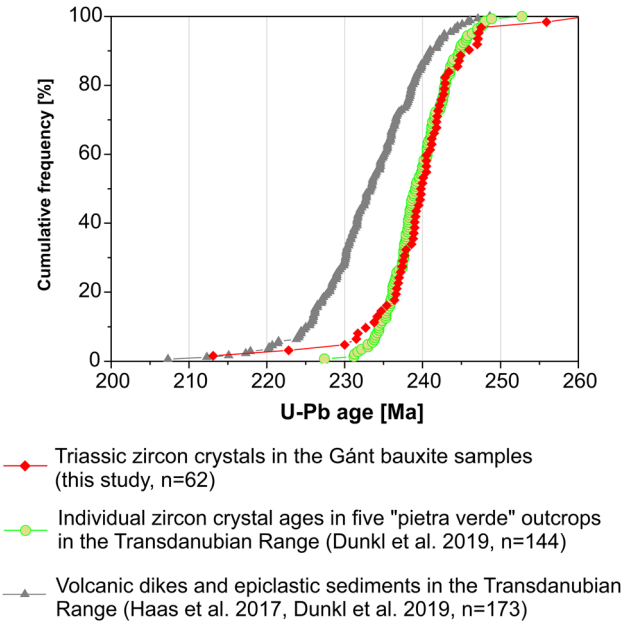

Fig. 9 Comparison of the Triassic zircon U–Pb ages detected in the Gánt Bauxite samples, the "pietra verde" tuff layers and the andesitic dikes plus the epiclastic sediments of the Transdanubian Range. The majority of the Triassic ages detected in the bauxite samples show perfect overlap with the "pietra verde" age data

Metamorphic formations with pre-Permian protoliths

The detected garnet, epidote, and the scarce appearance of kyanite, staurolite, xenotime and monazite indicate the exposure of amphibolite-facies metamorphic rocks in the source areas of the bauxite deposits and their cover strata. The closest outcrops of the metamorphic basement are located in the Velence Hills about 15 km from the Gánt locality (Fig. 1). However, the Variscan basement of the TR is composed of very low- and low-grade early Palaeozoic slate and phyllite. These formations are below the garnet, epidote and staurolite isograds and they are typically poor in zircon crystals (Lelkes-Felvári et al. 1994). Thus, for the detritus derived from metamorphic rocks, we have to consider more distant sources than the TR.

In the adjacent Eastern Alps, the Austroalpine metamorphic basement was exposed at a significantly larger area and the contemporaneous relief was probably more rugged than that of the TR (Dunkl et al. 2005). Thus, we consider the (proto-)Eastern Alps as a potential source of Paleogene clastic sediments of the TR. Another potential source area is the Bohemian Massif which is composed of igneous and metamorphic rocks and was exposed to erosion during the Eocene (Ziegler 1990). Figure 10 contains a compilation of zircon U–Pb ages that aims to describe the characteristic age signatures of the southern Eastern Alps and the southern Bohemian Massif. The composition of these data sets is

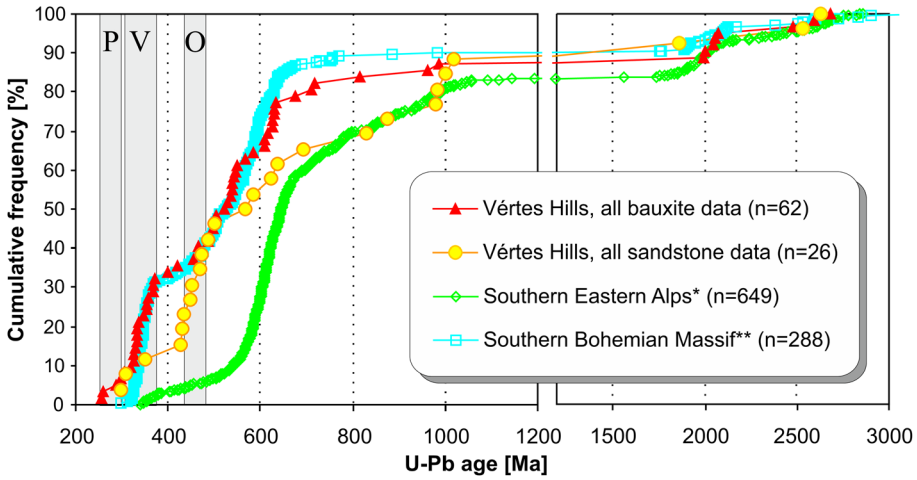

Fig. 10 Pre-Mesozoic zircon U–Pb ages detected in the bauxite and sandstone samples from the Vértes Hills compared to zircon ages of two potential source areas. The grey belts emphasize some relevant, diagnostic age ranges: P—Permian, V—Variscan, O—Ordovician. *The ages for the southern Eastern Alps are compiled from Siegesmund et al. (2021). The ages for the southern Bohemian Massif are from sand samples of modern rivers draining the Variscan and pre-Variscan basement (see Supplementary Data S6)

described in Supplementary Data S6. In the case of the Alps, we should keep in mind that the Penninic basement formations were not yet exposed to the surface implying that the proportion of the Variscan felsic formations was subordinate (< 5% of the zircon ages) compared to the schists containing mostly pre-Variscan zircons (Mandl et al. 2018; Haas et al. 2020; Siegesmund et al. 2021). That is the reason for the significant contrast to the age pattern from the Bohemian Massif (approx. 30% Variscan ages; Fig. 10), which at the time already exposes giant Variscan granitoid complexes besides the metamorphic rocks of pre-Carboniferous protoliths.

While the bauxite samples reveal pronounced matching with the southern Bohemian Massif, the sandstones from VH show less Variscan ages but a well-developed Ordovician age component appears (Fig. 10). This indicates more similarity to the Alpine age pattern, especially when considering that in the Southern Alps the Ordovician porphyry bodies were probably exposed already in Eocene time, which have relatively high zircon fertility (Söllner et al. 1997). Therefore, we suggest that the metamorphic-intrusive rocks of the south-eastern part of the Eastern Alps (and partly the Southern Alps) supplied the majority of the metamorphic detritus as well as most of the pre-Mesozoic zircons into the VH sandstones.

Stratigraphic implications of the new Paleogene U–Pb data

The new zircon U–Pb data allow to improve the chronostratigraphic constraints on the studied lacustrine-fluvial-lagoonal-marine assemblages and it is now possible to describe the evolution of the VH in more detail (Fig. 11).

The age component analysis yields highly consistent results for the Gánt Bauxite samples as follows: in all three samples, two age components appear at ~ 44 and 42 Ma. The similar age components indicate homogenous admixture within the sampled deposits of the Gánt area (Figs. 6 and 7). The U–Pb ages indicate that the Gánt Formation and thus the cover sequences are younger than previously estimated (Dunkl 1992; Kercsmár et al. 2008). However, a possible late Lutetian to early Bartonian formation age of the bauxite was already postulated based on biostratigraphic data of the cover (Kecskeméti 1998).

During the ~ 44–42 Ma period, the whole area was subject to denudation, which could represent a subtropical etchplain (Kaiser 1997). However, the U–Pb zircon age spectrum suggests that not all investigated karstic sinkholes were open and bauxite accumulation could happen only in a few depressions (i.e., at Gánt; Fig. 11a). During the Lutetian/Bartonian transition at ~ 41 Ma, just after the Gánt Bauxite deposition has ended, the Vértes Ridge could start to form and separate the NW and SE areas, which both were subjected to terrestrial to lagoonal clastic sedimentation with coal seams (Fig. 11b). New biostratigraphic data from Charophytes (Trabelsi et al. 2021) suggest a long period of deposition of the cover sequence over the whole of the Lutetian implying that the Gánt Bauxite might be as old as the earliest Lutetian. However, the precise U–Pb zircon ages of the Gánt Bauxite narrowed down the formation of the cover sequence to the late Lutetian (~ 42 Ma) to late Bartonian (~ 38 Ma) period. A major marine transgression within the Bartonian caused the almost complete flooding of the VH; along the highest paleotopography (the Vértes Ridge) platform carbonates formed while a shallow bathyal basin developed in the NW, and a shallower, mixed siliciclastic to carbonatic basin in the SE (Fig. 11c; Pálfalvi et al. 2006; Kercsmár et al. 2008). The new, independent geochronological data suggest that the uppermost strata of the Szőc Limestone were still deposited in the latest Bartonian, which is in agreement with former paleontological studies (Kollányi et al. 2003; Ozsvárt 2003) and recent Charophyte studies (Trabelsi et al. 2021). During this flooding, almost the complete area was covered by sediments, while some

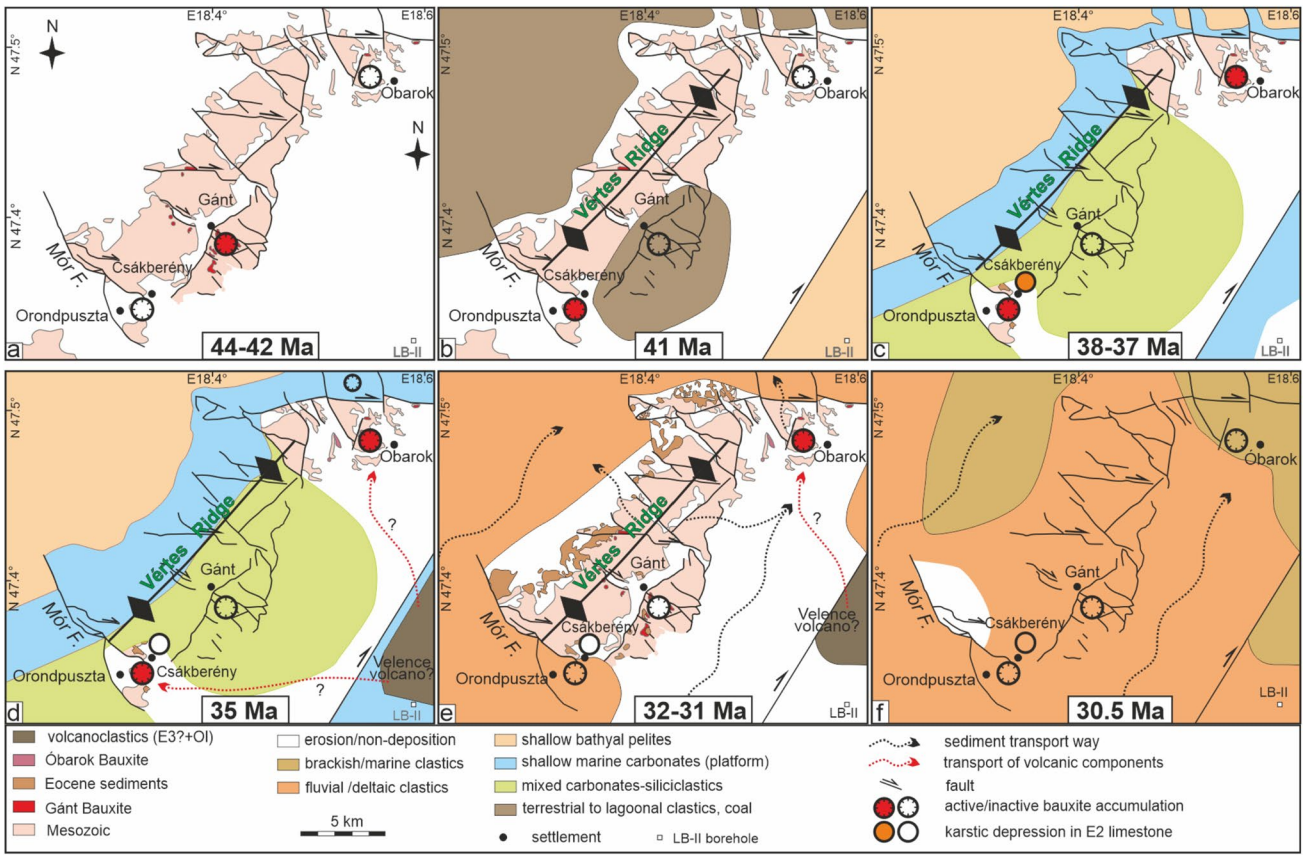

Fig. 11 Reconstruction of the palaeogeographic evolution of the Vértes Hills in six time slices between middle Eocene and early Oligocene. The present-day contour of the Mesozoic outcrops and the fault pattern can be used for orientation (see more details in Fig. 2a). For the reconstruction, the new age constraints were combined with the stratigraphic record revealed by the latest re-mapping of the area (Budai et al. 2008)

locally uplifted blocks witnessed ongoing bauxite sedimentation, i.e., Orondonpuszta on the SW and Óbarok on the NE (Fig. 11c).

The ~ 35 Ma age of bauxite formation at Orondpuszta points to a well-defined Priabonian bauxite accumulation event so far undetected in the s. s. TR (Fig. 11d). The results from this site underline the importance of detrital U–Pb zircon geochronology in establishing chronostratigraphic relations when paleontological data are not available or of poor resolution. Bauxite deposition happened in the SE when the carbonate platform of the Vértes Ridge prograded northwestward and the NW basin part could be still open. Local deformation events probably uplifted locally some areas along faults and controlled the local exposure and karstification of the Triassic rocks (e. g., Óbarok and Orondpuszta; Fig. 11d).

After uplift and regional denudation in the earliest Oligocene ('infra-Oligocene denudation' sensu Telegdi Roth 1927), the periphery of the VH subsided slowly and was covered by the fluvial Csatka Formation (Fig. 11e; Korpás 1981). The early Oligocene age of the Csatka Formation (the cover sand at Orondpuszta site) is now well defined (Fig. 12), with more reliability than the paleomagnetic or structural data used before (Fodor 2008; Sipos-Benkő et al. 2014) and is somewhat older than the estimated age of ~ 30 Ma in a nearby borehole (Danišík et al. 2015). During this time the Óbarok karstic dolines were open and accumulated weathering products (Fig. 11e).

The age of the bauxite formation at Óbarok was debated ever since the Oligocene tree trunk was recovered from the uppermost 2 m and used to estimate its stratigraphic position (Mindszenty et al. 2002). This is because the trunk might have been resedimented after the main bauxitic weathering event as a result of erosion of plant remnants from the surrounding karst terrain. The stratigraphic range of the trunk is also questionable. However, the new zircon U–Pb age data prove independently the early Oligocene bauxite formation event since the zircons were acquired from samples collected from the basal part of the Óbarok Bauxite. The new U–Pb age data of the Mány Member cover sand at Óbarok are in good agreement with the zircon distributions of the underlying bauxite and suggests

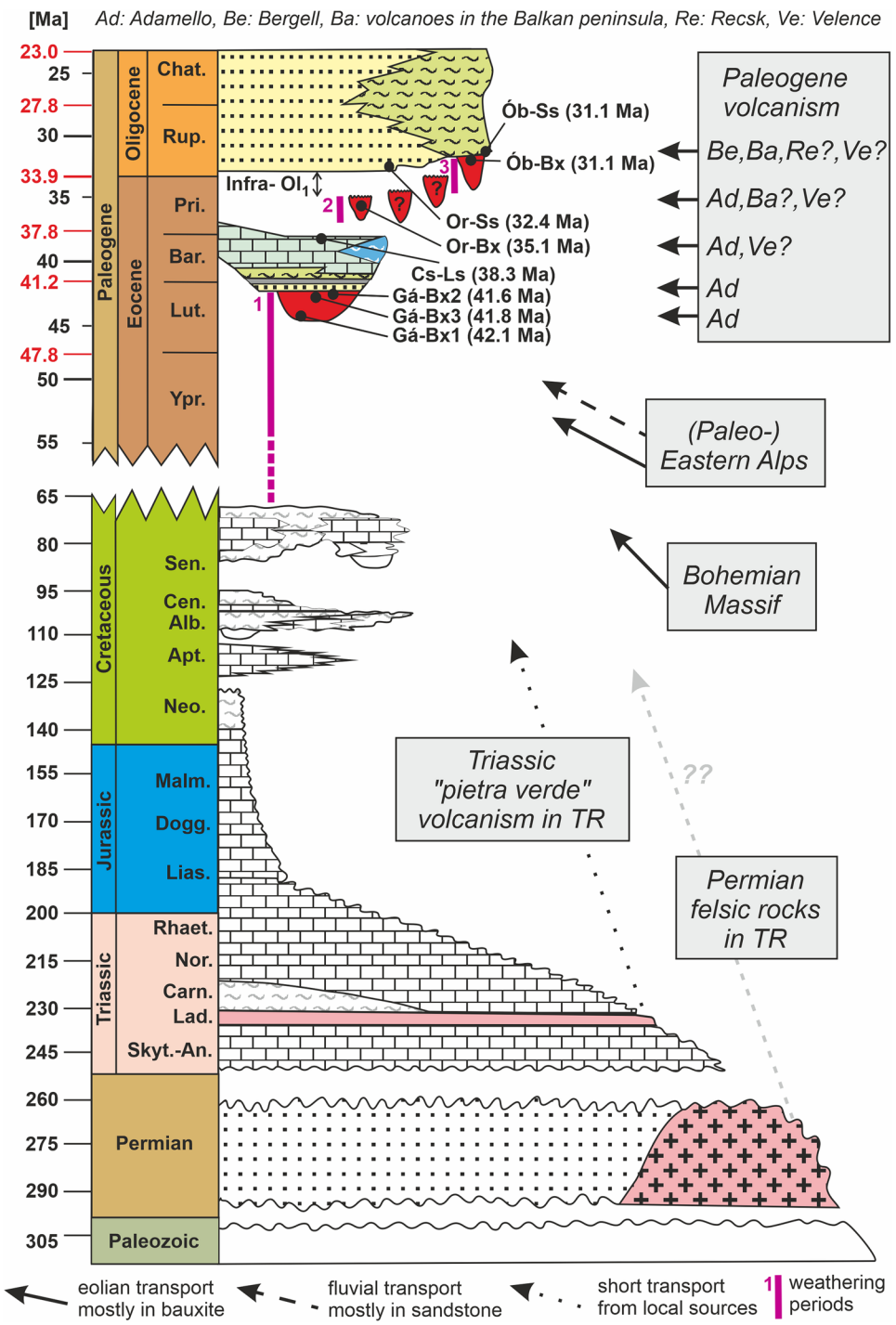

Fig. 12 Modified stratigraphy of the Vértes Hills area based on the new data obtained by this study. Gray rectangles indicate the possible sources and arrows the mode of transport of the detrital zircons. Ages in brackets refer to the youngest age components, i.e., the maximum age of deposition. The vertical magenta bars represent the identified bauxitic weathering periods. 'Infra-Ol_1' refers to the 'Infra-Oligocene' denudation period (Telegdhi 1927)

relatively continuous sedimentation (Figs. 5, 7, 12). The formation of the cover sequence can be correlated to the ongoing subsidence which was relatively fast during the middle part of the Oligocene, from ca. 31–28 Ma (Báldi 1986; Tari et al. 1993). The sedimentation of the VH remained dominantly fluvial but brackish intercalations occurred both in the NW (Tari et al. 1993) and in the eastern surroundings (Fig. 11f).

Timing of Paleogene ferrallitic weathering and denudation phases in Vértes Hills

Beyond the stratigraphic implications, the Paleogene zircon ages obtained from the VH samples allow the subdivision of alternating weathering-denudation and sedimentation phases recorded in the bauxitic sediments and the clastic and carbonate cover sequences, respectively, which could

be extrapolated to the entire TR or even to the Carpathian and the Eastern Alpine region. The ~ 44 and ~ 42 Ma age components detected in the Gánt Bauxite deposits indicate that the volcanogenic material could completely transform to bauxite in a relatively short time, until the development of the lacustrine cover. Thus, these ages mark the first well-dated Paleogene ferrallitic weathering period in the VH, which corresponds to the Middle Eocene Climatic Optimum peaking at 42–40 Ma (MECO; Zachos et al. 2008; Boscolo Galazzo et al. 2014; Westerhold et al. 2020). However, the onset of this first Paleogene bauxite formation period remains an open question due to the lack of Cretaceous to early Eocene volcanogenic zircon supply (Fig. 1).

The ~ 38 Ma age components in the Bartonian Cs-Ls sample define the maximum sedimentation age of the uppermost part of the Szőc Limestone and thus mark the oldest possible onset of the second Paleogene bauxitic weathering period. The local exposure of the Middle Eocene marine strata already in early Priabonian time is deduced from the presence of a ~ 20 m-thick sand layer in the Lb-II drillcore to the east of the VH deposited between middle and upper Eocene marine sequences (Kercsmár et al. 2008) (Fig. 10c). The U–Pb ages of the Orondpuszta bauxite assign this yet unknown bauxite formation period to the late Priabonian (maximum age of ~ 35 Ma), which corresponds to the last warm period before an eventual climate deterioration related to the early Oligocene glaciation around 33.5 Ma (e.g., Zachos et al. 2008; Westerhold et al. 2020). The ~ 35 Ma age can also be considered as the first geochronological evidence regarding the beginning of the so-called 'infra-Oligocene denudation'. Our data suggest that the denudation started already in the latest Eocene, instead of the early Oligocene as proposed by Telegdi-Roth (1927). The intense erosion, which resulted in the massive siliciclastic sediment transport from the Alps reached the VH no later than the earliest Oligocene as recorded in the ~ 32 Ma cover sediments (Csatka Formation) at the Orondpuszta site, which was affected by subsidence and basin formation during that time. This age also marks the end of the 'infra-Oligocene denudation', which now can be constrained between ~ 35 and ~ 32 Ma as suggested by our data (between the steps shown on Fig. 11d and e). At first, the denudation was restricted to locally elevated blocks, i.e., the bauxite deposits at Orondpuszta (~ 35 Ma), but became regional by the earliest Oligocene. The ~ 32 Ma maximum age of the Csatka Formation is coeval with the general increase of the sedimentation rate in the peri-Alpine basins (Kuhlemann et al. 2001). Since the Csatka Formation at Orondpuszta accumulated along a synsedimentary fault system, the ~ 32 Ma age also dates tectonic activity within the area. Seismic data indicate a strong connection to the possibly coeval Mór Fault at the SW boundary of the VH (Fig. 2a, N of the Orondpuszta site) along which the up to 800 m-thick Csatka Formation of Alpine origin accumulated (Fodor 2008; Selmeczi 2008). The apparent maximum age gap of ~ 3 Myr between the Orondpuszta bauxite and its siliciclastic cover sediments can correspond to the time span of the 'infra-Oligocene denudation', or might be represented, at least partially, by the coal seams present between the two formations.

The U–Pb ages of the Óbarok bauxite define the third intense, subaerial weathering period of the VH with a max. age of ~ 31 Ma, which may be related to a small warming interlude within the early Oligocene glaciation (e.g., Zachos et al. 2008). Afterall, since ferallitic weathering requires a hot humid climate, conditions must have been sufficiently warm and humid for an early Oligocene bauxite formation sustaining a subtropical flora (Mindszenty et al. 2002; Kocsis et al. 2014). Even though the two dated Priabonian and early Oligocene bauxite formation periods seem well separated in time, it is hard to rule out the possibility of several episodes of bauxite formation during the latest Eocene to early Oligocene time span. This could take place preferentially on elevated blocks (isolated from the coarse clastic supply of the Csatka Formation) over the entire period but the bauxites are only occasionally preserved (Fig. 12). Nevertheless, the Óbarok bauxite most likely represents the youngest ferallitic weathering period in the region, which continued at least until middle Rupelian time, i.e., beyond the onset of global cooling at the Eocene–Oligocene transition.

Implications for the late Eocene—early Oligocene palaeogeography (ca. 41–32 Ma)

Considering the new data, the original stratigraphical column (Fig. 2b) can be modified including the major elements of the provenance pattern (Fig. 12). Three modes of sediment transport are distinguished and allow for a detailed palaeogeographic reconstruction for the late Eocene to early Oligocene (Fig. 13).

Local sources

The erosional products derived from the TR experienced only short transport, most likely by minor, episodic and/or seasonally active creeks on the karstic surface. The most prominent local contribution to the bauxites is Middle Triassic zircons from the "pietra verde" tuffs. Moreover, reworked rare Permian zircons may derive from the post-Variscan felsic formations of the TR and a minor proportion of the older zircon grains may derive from the Palaeozoic formations exposed close to the VH.

Fluvial transport from the eastern Alps

The palinspastic reconstructions suggest that the TR occupied a more western position in Paleogene time, closer to the

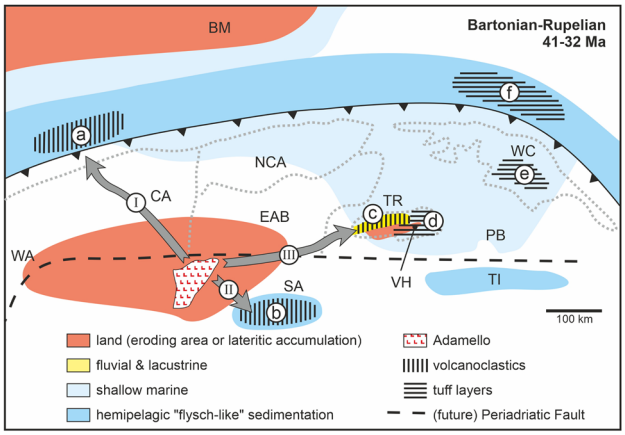

Fig. 13 Paleogeographic sketch-map of the Alpine-Carpathian-Pannonian region in late Eocene—early Oligocene. Grey dotted lines are the contours of the palinspastically restored Eastern Alps, Transdanubian Range and Western Carpathians from Frisch et al. (1998) and Kázmér et al. (2003). Positions of the Adamello and the Northern and Southern Alpine flysch deposits are taken from Lu et al. (2018). Arrows indicate the major radial river systems draining the exhuming and uplifting Alps (I and II) and the axial 'paleo-Drau River' that delivered volcanoclastic detritus to the Transdanubian Range (III). The vertical and horizontal patterns distinguish volcanoclastic materials that experienced fluvial transport as siliciclastic detritus or aeolian transport as volcanic ash, respectively. A significant contribution of Variscan zircons most likely arrived at the Transdanubian Range via aeolian transport from the Bohemian Massif, widely exposed during the Eocene as part of the European Platform (Kováč et al 2016). *RBH* Rhenish-Bohemian Highlands, *CA* Central Alps, *EAB* Eastern Alpine Basement, *NCA* Northern Calcareous Alps, *PB* Pannonian Basin, *SA* Southern Alps, *TI* Tisza Unit, *TR* Transdanubian Range, *VH* Vértes Hills, *WA* Western Alps, *WC* Western Carpathians. **a** Taveyannaz flysch basin, **b** Trentino basin (Lu et al. 2018), **c** siliciclastic Oligocene in the Transdanubian Range (Benedek et al. 2001), **d** Paleogene tuff layers reworked on the karstic plateaus and preserved in the marine, fine-grained successions (Báldi 1984; Dunkl 1992, this study), **e**, **f** tuff layers in the Central-Carpathian Basin and in the Magura nappe (Soták 2010; Van Couvering et al. 1981)

present-day Eastern Alps (e.g., Kázmér and Kovács 1985; Schmid et al. 2008; Héja et al. 2018). For the origin and provenance of the high amount of Oligocene siliciclastic sediments of the TR Korpás (1981) proposed an eastward flowing palaeoriver system originating in the Eastern Alps, which is underlined by the petrographical, mineralogical, geochemical and thermochronological data of Benedek et al. (2001). The pre-Mesozoic U–Pb ages of the VH sandstone samples further support such provenance (Fig. 10; for an explanation of the higher proportion of Ordovician ages see Sect. "Metamorphic formations with pre-Permian protoliths"). The eastward transport of Paleogene volcanoclastic material and detritus from the Eastern Alpine metamorphic basement is assigned to the "palaeo-Drau" river system.

Placing the VH data in a wider context allows for depicting the late Eocene to early Oligocene denudation pattern of the proto-Alps, and to distinguish the volcanoclastic-bearing formations by their mode of transport (Fig. 13). Beyond the radial river systems that transported the eroded sediment from the emerging Alps to the northern- and southern Alpine foreland basins, the tectonically already active Periadriatic Fault (Figs. 1 and 13) generated a weak zone giving way to the palaeo-Drau River that fed the basins in the TR. In our reconstruction, the airborne tuff and volcaniclastic layers in fluvial and marine deposits of these basins are distinguished from the airborne, but later bauxitized sediments in the karstic depressions (Fig. 13).

Aeolian transport from the Bohemian Massif and the coeval volcanoes

The scarce rounded ultrastable heavy minerals and pre-Eocene zircons in the bauxite deposits indicate the lack of massive contributions by fluvial transport from exposed basement areas. It also implies that the karstic surfaces with bauxite formation in Paleogene time in the VH constituted elevated positions above the surrounding basins filled by rivers or by marine sedimentation. It is thus highly plausible that the major mass of the primary sediment of the bauxite arrived at the karstic dolines by aeolian transport. This kind of transport is obvious in the case of the Paleogene mainly euhedral zircons from synsedimentary volcanic eruptions and proven by the intact tuff layers preserved in fine-grained sediments of the marine sequences of the region (Báldi 1984).

To identify the potential sources of the pre-Mesozoic zircons of the bauxites, a comparison of the zircon ages obtained from the sandstone and bauxite samples is crucial (Fig. 10). The Alpine source for the bauxitic sediments, as proposed for the Oligocene sandstones, is contradicted by their high proportion of Variscan zircon content. The Bohemian Massif represents the present-day exposed part of the Rhenish-Bohemian Highlands that emerged along the southern margin of the European continent in Eocene time (Kováč et al. 2016). The abundance of Variscan felsic igneous formations and amphibolite facies metamorphic rocks with early Palaeozoic and even older protoliths within the Bohemian Massif matches well to the zircon age spectra obtained in the bauxites (Fig. 10). The derivation of detritus from the European continent by fluvial transport was impossible, as the Alpine-Carpathian-Pannonian micro-continent assemblage, including the VH, was separated from the Rhenish-Bohemian Highlands by a marine domain, the Alpine-Carpathian foreland system (e.g., Kováč et al. 2016) (Fig. 13). Thus, we propose that beyond the volcanic ashes, also pre-Permian (especially Variscan) igneous-metamorphic material from the Bohemian Massif reached the karstic areas by aeolian transport.

Conclusions

- According to the detrital zircon U–Pb age spectra and the heavy mineral content the precursor material of the bauxite deposits of the Vértes Hills and their siliciclastic covers have the following four major sources: (i) the Middle Triassic "pietra verde" bentonitic tuff and minor subvolcanic bodies that are a part of the underlying carbonate sequence, (ii) metamorphic detritus from the Eastern Alps, (iii) metamorphic and Variscan igneous rocks from the Bohemian Massif or other parts of the currently covered European Rhenish-Bohemian Highlands and (iv) from the coeval Paleogene volcanism in the Alps and probably also from volcanoes of the Balkan peninsula and the Pannonian Basin. Palaeozoic formations of the Transdanubian Range, i.e., the Permian felsic igneous rocks, might supplied some minor amount of siliciclastic material.
- While the subsequently bauxitized magmatic and metamorphic materials reached the emerged karstic plateaus mostly by aeolian transport, the components of the Oligocene sandstone cover layers were transported by rivers during the initial subsidence of the formerly elevated plateaus.
- The new provenance indicators allow for refining the late Eocene—early Oligocene paleogeographic reconstruction of the Alpine-Pannonian region and emphasize the significance of east-directed sediment transport. Moreover, we outline a new scheme for the distinction of airborne tuff layers, bauxitic sediment, and fluvially transported volcanoclastic sequences.
- U–Pb age components of the zircon crystals from Paleogene ashfall events preserved in the bauxitic sequences constrain the timing of deposition and the periods of intense ferallitic weathering. The Paleogene palaeogeographic evolution of the Vértes Hills can be described in six detailed time slices from 44 to 31 Ma.
- The humid tropical to subtropical conditions required for the formation of bauxitic deposits must have prevailed in the studied area until at least 31 Ma, i.e., beyond the onset of global cooling at the Eocene-Oligocene transition.

Supplementary Information The online version contains supplementary material available at https://doi.org/10.1007/s00531-022-02249-3.

Acknowledgements This project was part of a Ph.D. program supported by the Doctoral School of Earth Sciences, Eötvös Loránd University, Budapest. Analytical work has been performed at the Geoscience Center Göttingen. Additional financial input was provided by the ERASMUS+ Internship program (contract number: 18/1/KA103/047073/SMP), the Hungarian Scientific Research Fund (ID: K106197 and K134873) and the Papp Simon Foundation. The authors are grateful to András Rózsahegyi for granting access to the former Óbarok open pit, currently under recultivation. Special thanks to Andreas Kronz, Kirsten Techmer, Judit Nagy, Irina Ottenbacher, Cornelia Friedrich and László Szikszay for help with various analytical and sample preparation procedures and Ildikó Selmeczi for professional discussions. We deeply appreciate the thoughtful comments by Michael Wagreich and an anonymous reviewer as well as journal editor Ulrich Riller.

Funding Open access funding provided by Eötvös Loránd University.

Declarations

Conflict of interest The authors declare no conflict of interest.

References

Arató R, Dunkl I, Takács Á, Szebényi G, Gerdes A, von Eynatten H (2018) Thermal evolution in the exhumed basement of a stratovolcano: case study of the Miocene Mátra Volcano, Pannonian Basin. J Geol Soc 175:820–835. https://doi.org/10.1144/jgs2017-117

Balázs A, Matenco L, Magyar I, Horváth F, Cloetingh SAPL (2016) The link between tectonics and sedimentation in back-arc basins: new genetic constraints from the analysis of the Pannonian Basin. Tectonics 35(6):1526–1559

Báldi T (1984) The terminal Eocene and Early Oligocene events in the Hungary and the separation of an anoxic, cold Paratethys. Eclogae Geol Helv 77(1):1–27

Báldi T (1986) Mid-tertiary stratigraphy and Paleogeographic evolution of Hungary. Akadémiai Kiadó, Budapest p 201

Báldi-Beke M (1984) The nannoplankton of the Transdanubian Palaeogene formations. Geol Hung Ser Palaeontol 43:307

Báldi-Beke M (2003) Stratigraphy and palaeoecology of the formations overlying the Middle Eocene coal sequence based on nannofossils - (Transdanubia, Hungary). Bull Hung Geol Soc 133(3):325–344

Báldi-Beke M, Báldi T (1985) The evolution of the Hungarian Palaeogene basins. Acta Geol Hung 28:5–28

Bárdossy G, Aleva GJJ (1990) Lateritic Bauxites. Dev Econ Geol 27, Elsevier p 624

Bárdossy G (2010) The Szőc bauxite deposit. Occasional Papers Geol Inst Hung 211, Budapest p 126

Bárdossy G (2013) Karst Bauxites. Elsevier p 441

Barth S, Felix O, Martin M (1989) U-Th–Pb systematics of morphologically characterized zircon and allanite: a high-resolution isotopic study of the Alpine Rensen pluton (northern Italy). Earth Planet Sci Lett 95(3–4):235–254

Beltrán-Triviño A, Winkler W, von Quadt A, Gallhofer D (2016) Triassic magmatism on the transition from Variscan to Alpine cycles: evidence from U-Pb, Hf, and geochemistry of detrital minerals. Swiss J Geosci 109(3):309–328

Benedek K (2002) Paleogene igneous activity along the easternmost segment of the Periadriatic-Balaton Lineament. Acta Geol Hung 45(4):359–371

Benedek K, Nagy Z, Dunkl I, Szabó C, Józsa S (2001) Petrographical, geochemical and geochronological constraints on igneous clasts and sediments hosted in the Oligo-Miocene Bakony Molasse, Hungary: evidence for a Paleo-Drava River system. Int J Earth Sci 90(3):519–533

Benedek K, Pécskay Z, Szabó C, Jósvai J, Németh T (2004) Paleogene igneous rocks in the Zala Basin (Western Hungary): link to the Paleogene magmatic activity along the Periadriatic Lineament. Geol Carpathica 55(1):43–50

Bergomi MA, Zanchetta S, Tunesi A (2015) The Tertiary dike magmatism in the Southern Alps: geochronological data and geodynamic significance. Int J Earth Sci 104(2):449–473

Bernhardt B (1990) Eocén. In: Bence G, Bernhardt B, Bihari D, Bálint C, Császár G, Gyalog L, Haas J, Horváth I, Jámbor Á, Kaiser M, Kéri T, Kókay J, Konda J, Lelkesné-Felvári G, Majoros G, Peregi Z, Raincsák G, Solti G, Tóth Á, Tóth G: Geology of the Bakony Mountains (Hungary). Geol Inst Hung, Budapest, pp 49–53

Bignot G, Blondeau A, Guernet C, Perreau M, Poignant A, Renard M, Riveline J, Gruas C, Dudich E, Kazmer M, Kopek G (1985) Age and characteristics of the Eocene transgression at Gánt (Vértes Mts, Transdanubia, Hungary). Acta Geol Hung 28:29–48

Birkeland PW (1984) Soils and Geomorphology. Oxford University Press p, New York, p 372

Boev B, Yanev Y (2001) Tertiary magmatism within the Republic of Macedonia: a review. Acta Vulcanol 13(1–2):57–71

Boni M, Reddy SM, Mondillo N, Balassone G, Taylor R (2012) A distant magmatic source for Cretaceous karst bauxites of southern Apennines (Italy), revealed through SHRIMP zircon age dating. Terra Nova 24(4):326–332

Böröczky T (1996) Jelentés az Óbarok XI. bauxittelepen végzett kutatómunka és készletszámítás eredményéről (Report on the exploration and reserves' calculation of the Óbarok XI. bauxite deposit). Bauxite Prospecting Company, manuscript report (in Hungarian)

Boscolo Galazzo F, Thomas E, Pagani M, Warren C, Luciani V, Giusberti L (2014) The middle Eocene climatic optimum (MECO): a multiproxy record of paleoceanographic changes in the southeast Atlantic (ODP Site 1263, Walvis Ridge). Paleoceanography 29:1–19

Brügel A, Dunkl I, Frisch W, Kuhlemann J, Balogh K (2000) The record of Periadriatic volcanism in the Eastern Alpine Molasse zone and its paleogeographic implications. Terra Nova 12:42–47

Budai T, Vörös A (2006) Middle Triassic platform and basin evolution of the southern Bakony Mountains (Transdanubian Range, Hungary). Riv Ital Paléontol Stratigr 112(3):359–371

Budai T, Császár G, Csillag G, Dudko A, Koloszár L, Majoros G (1999) Geology of the Balaton Highland. Explanatory notes to the Geological map of the Balaton Highland. Occasional Papers Geol Inst Hung, Budapest

Budai T, Császár G, Csillag G, Fodor L, Gál N, Kercsmár Zs, Kordos L, Pálfalvi S, Selmeczi I (2008) Geology of the Vértes Hills. Explanatory book to the Geological Map of the Vértes Hills 1:50000. Geol Inst Hung, Budapest p 368

Carannante G, Mindszenty A, Neumann AC, Rasmussen KA, Simone L, Tóth K (2004) Inland blue-hole type ponds in the Mesozoic karst-filling sequences. Abstracts, 15th IAS Regional Meeting, April, 1994, Ischia, Italy, 102–103

Comer JB (1974) Genesis of Jamaican bauxite. Econ Geol 69(8):1251–1264

Comer JB, Naeser CW, McDowel FW (1980a) Fission-track ages of zircon from Jamaican bauxite and Terra Rossa. Econ Geol 75:117–121

Comer JB, Naeser CW, McDowell FW (1980b) Fission-track ages of zircon from Jamaican bauxite and terra rossa. Econ Geol 75(1):117–121

Császár G (1986) Middle Cretaceous formations of the Transdanubian Central Range: stratigraphy and connection with bauxite genesis. Geol Hung Ser Geol 23, Budapest p 295

Csillag G, Sebe K (2015) Long-term geomorphological evolution. In: Lóczy D (ed) Landscapes and Landforms of Hungary. Springer, pp 29–38

Csontos L, Nagymarosy A, Horváth F, Kováč M (1992) Tertiary evolution of the Intra-Carpathian area: a model. Tectonophysics 208:221–241. https://doi.org/10.1016/0040-1951(92)90346-8

Cvetković V, Šarić K, Pécskay Z, Gerdes A (2016) The Rudnik Mts. volcano-intrusive complex (central Serbia): an example of how magmatism controls metallogeny. Geol Croat 69(1):89–99. https://doi.org/10.4154/gc.2016.08

D'Argenio B, Mindszenty A (1995) Bauxites and related paleokarst: tectonics and climatic event markers at regional unconformities. Ecolg Geol Helv 88:453–499

Danišík M, Fodor L, Dunkl I, Gerdes A, Csizmeg J, Hámor-Vidó M, Evans NJ (2015) A multi-system geochronology in the Ad-3 borehole, Pannonian Basin (Hungary) with implications for dating volcanic rocks by low-temperature thermochronology and for interpretation of (U–Th)/He data. Terra Nova 27(4):258–269

Dennen WH, Norton HA (1977) Geology and geochemistry of bauxite deposits in the lower Amazon basin. Econ Geol 72(1):82–89

Di Capua A, Barilaro F, Groppelli G (2021) Volcanism and volcanogenic submarine sedimentation in the Paleogene Foreland Basins of the Alps: reassessing the source-to-sink systems with an actualist view. Geosciences 11(1):23. https://doi.org/10.3390/geosciences11010023

Dudich E, Gy Komlóssy (1969) Considerations paleogeographiques et tectoniques sur le probléme de l'age des bauxites. Boll Soc Geol Hung 98(2):155–165

Dunkl I (1992) Origin of Eocene-covered karst bauxites of the Transdanubian Central Range (Hungary): evidence for early Eocene volcanism. Eur J Min 4:581–596

Dunkl I, Kuhlemann J, Reinecker J, Frisch W (2005) Cenozoic relief evolution of the Eastern Alps—constraints from apatite fission track age-provenance of Neogene intramontane sediments. Austrian J Earth Sci 98:92–105

Dunkl I, Farics É, Józsa S, Lukács R, Haas J, Budai T (2019) Traces of Carnian volcanic activity in the Transdanubian Range, Hungary. Int J Earth Sci 108:1451–1466. https://doi.org/10.1007/s00531-019-01714-w

Fodor L (2008) Structural geology. In: Budai T, Fodor L (ed) Explanatory Book to the Geological Map of the Vértes Hills (1:50 000). Geological Institute of Hungary, Budapest pp 282–300

Frei D, Gerdes A (2009) Precise and accurate in situ U-Pb dating of zircon with high sample throughput by automated LA-SF-ICP-MS. Chem Geol 261:261–270

Frisch W, Kuhlemann J, Dunkl I, Brügel A (1998) Palinspastic reconstruction and topographic evolution of the Eastern Alps during late Tertiary tectonic extrusion. Tectonophysics 297:1–15

Góczán F, Pataki A, Rákosi L, Tiszay J (2002) Albaian bauxite depositing in the Halimba basin). Földtani Kutatás 39(1):50–52

Guynn J, Gehrels G (2010) Comparison of detrital zircon age distributions using the K-S Test, Arizona LaserChron Center, University of Arizona, https://sites.google.com/a/laserchron.org/laserchron/home (15–11–2013).

Gyalog J (2005) Explanatory notes to the geological map of Hungary – 1:100 000. Geol Inst Hun, Budapest
Gyalog L, Horváth I (2004) Geology of the Velence Hills and the Balatonfő. Explanatry Book of the Geological Map of the Velence Hills (1:25 000) and the Geological Map of the Pre-Sarmatian Surface of the Balatonfő–Velence Area (1:100 000). Geol Inst Hun, Budapest
Haas J (1983) Senonian cycle in the Transdanubian Central Range. Acta Geol Hung 26(1–2):21–40
Haas J (1991) Tectonic and eustatic control of bauxite formation in the Transdanubian Central Range (Hungary). Acta Geol Hung 34(3):253–262
Haas J, Budai T (1995) Upper Permian-Triassic facies zones in the Transdanubian Range. Riv Ital Paleont Strat 101(3):249–266
Haas J, Kovács S, Krystyn L, Lein R (1995) Significance of Late Permian-Triassic facies zones in terrane reconstructions in the Alpine-North Pannonian domain. Tectonophysics 242:19–40
Haas J, Budai T, Dunkl I, Farics É, Józsa S, Kövér S, Götz AE, Piros O, Szeitz P (2017) The Budaörs-1 well revisited: contributions to the Triassic stratigraphy, sedimentology, and magmatism of the southwestern part of the Buda Hills. Central Eur Geol 60:201–229. https://doi.org/10.1556/24.60.2017.008
Haas I, Eichinger S, Haller D, Fritz H, Nievoll J, Mandl M et al (2020) Gondwana fragments in the Eastern Alps: a travel story from U/Pb zircon data. Gondwana Res 77:204–222
Hably L, Erdei B, Selmeczi I (2015) A late Oligocene (Egerian) flora from Környe, near Tatabánya, N Hungary. Neues Jahrbuch für Geologie und Paläontologie Abhandlungen. https://doi.org/10.1127/njgpa/2015/0487
Héja G, Kövér S, Csillag G, Németh A, Fodor L (2018) Evidences for pre-orogenic passive-margin extension in a Cretaceous fold-and-thrust belt on the basis of combined seismic and field data (western Transdanubian Range, Hungary). Int J Earth Sci 107(8):2955–2973
Jackson SE, Pearson NJ, Griffin WL, Belousova EA (2004) The application of laser ablation inductively coupled mass spectrometry to in situ U-Pb zircon geochronology. Chem Geol 211:47–69
Ji WQ, Wu FY, Tiepolo M, Langone A, Braga A (2013) Zircon U–Pb age and Hf isotope constraints on the petrogenesis of the Alpine Peri-Adriatic intrusions. Min Mag 77:1386
Ji WQ, Malusà MG, Tiepolo M, Langone A, Zhao L, Wu FY (2019) Synchronous Periadriatic magmatism in the Western and Central Alps in the absence of slab breakoff. Terra Nova 31(2):120–128
Kaiser M (1997) A geomorphic evolution of the Transdanubian Mountains, Hungary. Z Geomorphol N.F. 110:1–14
Kázmér M, Kovács S (1985) Permian-Paleogene paleogeography along the eastern part of the Insubric-Periadriatic lineament system: evidence for continental escape of the Bakony-Drauzug unit. Acta Geol Hung 28(1–2):71–84
Kázmér M, Dunkl I, Frisch W, Kuhlemann J, Ozsvárt P (2003) The Paleogene forearc basin of the Eastern Alps and Western Carpathians: subduction erosion and basin evolution. J Geol Soc 160:413–428
Kecskeméti T (1998) Magyarország epikontinentális eocén képződményeinek rétegtana (Stratigraphy of the Eocene epicontinental formations of Hungary, in Hungarian) — In: Bérczi I, Jámbor Á (eds): Magyarország geológiai képződményeinek rétegtana (The geological formations of Hungary, in Hungarian). Mol Rt, Hung Geol Inst, Budapest pp 403–418
Kelemen P, Dunkl I, Csillag G, Mindszenty A, von Eynatten H, Józsa S (2017) Tracing multiple resedimentation on an isolated karstified plateau: the bauxite-bearing Miocene red clay of the Southern Bakony Mountains, Hungary. Sediment Geol 358:84–96
Kelemen P, Csillag G, Dunkl I, Mindszenty A, Kovács I, von Eynatten H, Józsa S (2021) Terrestrial kaolin deposits trapped in Miocene karstic sinkholes on planation surface remnants, Transdanubian Range, Pannonian Basin (Hungary). Geol Mag 158(2):349–358
Kercsmár Z (2018) Eocene. In: Budai T. (eds) Geology of the Gerecse Mountains. Regional map series of Hungary. Explanatory Book to the Geological Map of the Gerecse Mountains (1: 50 000). Mining and Geological Survey of Hungary 57–106
Kercsmár Z, Pálfalvi S, Less G, Kordos L (2008) Eocene (Cenozoic). In: Budai T., Fodor L. (eds.): Geology of the Vértes Hills. Explanatory book to the Geological Map of the Vértes Hills 1:50000. Geological Institute of Hungary, Budapest pp 58–80
Kiss J (1955) Recherches sur les bauxites de la Hongrie. I Gánt Acta Geol Hung 3:45–58
Kocsis L, Ozsvárt P, Becker D, Ziegler R, Scherler L, Codrea V (2014) Orogeny forced terrestrial climate variation during the late Eocene–early Oligocene in Europe. Geology 42(8):727–730
Kókay J, Hamor T, Lantos M, Müller P (1989) The paleomagnetic and geological study of borehole section Berhida 3. Ann Rep Hung Geol Inst 45–63
Kollányi K, Bernhardt B, Báldiné-Beke M, Lantos M (2003) Integrated stratigraphic examination of the Eocene boreholes in Transdanubia. Bull Hung Geol Soc 131(1):69–90
Komlóssy G (1967) Contribution a la connaissance de la genese des bauxites hongroises. Acta Geol Acad Sci Hung 11(4):477–489
Korpás L (1981) Oligocene and Lower Miocene Formations of the Transdanubian Range. Ann Geol Inst Hung 64:1–140
Kováč M, Plašienka D, Soták J, Vojtko R, Oszczypko N, Less G, Vlasta Ć, Bernhard F, Králiková S (2016) Paleogene palaeogeography and basin evolution of the Western Carpathians, Northern Pannonian domain and adjoining areas. Glob Planet Change 140:9–27
Kövér S, Fodor L, Haas J, Klötzli U, Szabó C, Zajzon N (2018) Evidence for Late Triassic acidic volcanism in the Neotethyan region: U/Pb zircon ages from Jurassic redeposited clasts and their geodynamic implication. Int J Earth Sci 107(8):2975–2998. https://doi.org/10.1007/s00531-018-1638-2
Kuhlemann J, Frisch W, Dunkl I, Székely B (2001) Quantifying tectonic versus erosive denudation. The Miocene core complexes of the Alps. Tectonophysics 330:1–23. https://doi.org/10.1016/S0040-1951(00)00209-2
Lelkes-Felvári G, Sassi R, Zirpoli G (1994) Lithostratigraphy and Variscan metamorphism of the Paleozoic sequences in the Bakony Mountains, Hungary. Mem Sci Geol 46:303–312
Lu G, Winkler W, Rahn M, von Quadt A, Willett SD (2018) Evaluating igneous sources of the Taveyannaz formation in the Central Alps by detrital zircon U-Pb age dating and geochemistry. Swiss J Geosci 111:399–416
Mandl M, Kurz W, Hauzenberger C, Fritz H, Klötzli U, Schuster R (2018) Pre-Alpine evolution of the Seckau Complex (Austroalpine basement/Eastern Alps): Constraints from in-situ LA-ICP-MS UPb zircon geochronology. Lithos 296:412–430
Mange MA, Maurer HF (1992) Heavy Minerals in Colour. Chapman & Hall, 2–6 Boundary Row, London p 147
Marchand E, Séranne M, Bruguier O, Vinches M (2021) LA-ICP-MS dating of detrital zircon grains from the Cretaceous allochthonous bauxites of Languedoc (south of France): Provenance and geodynamic consequences. Basin Res 33(1):270–290
Marchev P, Raicheva R, Downes H, Vaselli O, Chiaradiad M, Moritz R (2004) Compositional diversity of Eocene-Oligocene basaltic magmatism in the Eastern Rhodopes, SE Bulgaria: implications for genesis and tectonic setting. Tectonophysics 393:301–328
Mindszenty A (1969) Ore geology, mineralogy and geochemistry of the Újbarok–Vázsonypuszta bauxite deposits. Unpublished manuscript, Institute of Geography and Geology, Eötvös Loránd University, Budapest
Mindszenty A (2010) Bauxite deposits of Gánt (Vértes Hills, Hungary). Acta Min-Petrogr Field Guide Ser 11:11

Mindszenty A, Szőts A, Horváth A (1989) Excursion A3: Karstbauxites in the Transdanubian Mid-Mountains. Guidebook, IAS 10th Regional Meeting, Budapest, 11–48

Mindszenty A, Gál-Sólymos K, Csordás-Tóth A, Imre I, Felvári G (1991) Extraclasts from Cretaceous/Tertiary bauxites of the Transdanubian Central Range and the Northern Calcareous Alps. Preliminary results and tentative geological interpretation. Jubiläumsschrift 20 Jahre geologische Zusammenarbeit Österreich–Ungarn 309–345

Mindszenty A, Csoma A, Török Á, Hips K, Hertelendi E (2000) Rudistid limestones, bauxites, paleokarst and geodynamics. The case of the Cretaceous of the Transdanubian Range. Bull Hung Geol Soc 131(1–2):107–152

Mindszenty A, Böröczky T, Rákosi L, Weiszburg T (2002) Investigation of a mineralized tree trunk in the Óbarok bauxite deposit. Földtani Kutatás 39(1):53–55

Mundil R, Brack P, Meier M, Rieber H, Oberli F (1996) High resolution U-Pb dating of Middle Triassic volcaniclastics: Time-scale calibration and verification of tuning parameters for carbonate sedimentation. Earth Planet Sci Lett 141(1–4):137–151

Nagymarosy A, Báldi-Beke M (1988) The position of the Paleogene Formations of Hungary in the standard nannoplankton zonation. Ann Univ Scient Bp Rolando Eötvös Nomin Sect Geol 28:3–25

Nemecz E, Varjú G (1967) Relationship between „Flintclay" and bauxite formation in the Pilis Mountains. Acta Geol Acad Sci Hung 11(4):453–476

Neubauer F, Heberer B, Dunkl I, Liu X, Bernroider M, Dong Y (2018) The Oligocene Reifnitz tonalite (Austria) and its host rocks: implications for Cretaceous and Oligocene-Neogene tectonics of the south-eastern Eastern Alps. Geol Carp 69(3):237–253

Olšavský M (2001) Evidence of volcanism in the Middle Triassic Reifling Limestones of the Hronikum Unit. Geolines 13:97–98

Ozsvárt P (2003) A magyarországi paleogén medence paleo-oceanográfiája bentosz foraminiferák ökológiai vizsgálatai alapján (Paleo-oceanography of the Hungarian Paleogene basin based on the ecological investigation of benthos foraminifera, in Hungarian). Ph.D. Manuscript, ELTE Dept of Paleontol, Budapest p 182

Pálfalvi S (2007) Reconstruction of Eocene depositional environments in the Vértes Hills, based on microfacies analysis. Unpublished PhD Thesis, Eötvös University, Budapest, Hungary

Pálfalvi S, Fodor L, Kercsmár Zs, Báldi-Beke M, Kollányi K, Less Gy (2006) Sedimentation pattern, tectonic control, and basin evolution of the northern Transdanubian Eocene basins (Vértes Hills, central Hungary). Geophys Res Abstr 8, EGU06-A-08384 /Sref-ID:1607–7962/gra/ (European Geosciences Union General Assembly, Vienna).

Pálfy J, Parrish RR, David K, Vörös A (2003) Mid-Triassic integrated U-Pb geochronology and ammonoid biochronology from the Balaton Highland (Hungary). J Geol Soc 160:271–284

Pamić J, Balen D (2001) Tertiary magmatism of the Dinarides and the adjoining South Pannonian Basin: an overview. Acta Vulcanol 13(1–2):9–24

Pfiffner AQ (2014) Geology of the Alps. West Sussex, Wiley pp 140–165

Pomella H, Klötzli U, Scholger R, Stipp M, Fügenschuh B (2011) The Northern Giudicarie and the Meran-Mauls fault (Alps, Northern Italy) in the light of new paleomagnetic and geochronological data from boudinaged Eo-/Oligocene tonalites. Int J Earth Sci 100:1827–1850

Press WH, Teukolsky SA, Vetterling WT, Flannery BP (1986) Numerical recipes: The art of scientific computing. Cambridge University Press, p 848

Retallack GJ (1990) Soils of the past. Unwin-Hyman, Boston

Romer RL, Siegesmund S (2003) Why allanite may swindle about its true age. Contrib Mineral Petrol 146:297–307. https://doi.org/10.1007/s00410-003-0494-6

Rosenberg CL (2004) Shear zones and magma ascent: a model based on a review of the Tertiary magmatism in the Alps. Tectonics 23(3)

Rostási Á, Raucsik B, Varga A (2011) Paleoenvironmental controls on the clay mineralogy of Carnian sections from the Transdanubian Range (Hungary). Palaeo Palaeo Palaeo 300:101–112

Samperton KM, Schoene B, Cottle JM, Keller CB, Crowley JL, Schmitz MD (2015) Magma emplacement, differentiation and cooling in the middle crust: Integrated zircon geochronological–geochemical constraints from the Bergell Intrusion, Central Alps. Chem Geol 417:322–340. https://doi.org/10.1016/j.chemgeo.2015.10.024

Schaltegger U, Brack P, Ovtcharova M, Peytcheva I, Schoene B, Stracke A, Marocchi M, Bargossi GM (2009) Zircon and titanite recording 1.5 million years of magma accretion, crystallization and initial cooling in a composite pluton (southern Adamello batholith, northern Italy). Earth Planet Sci Lett 286:208–218. https://doi.org/10.1016/j.epsl.2009.06.028

Scharbert S (1975) Radiometrische Altersbestimmungen von Intrusivgesteinen im Raum Eisenkappel (Karawanken, Kärnten). Verhandlungen Der Geologischen Bundesanstalt 4:301–304

Schefer S, Cvetković V, Fügenschuh B, Kounov A, Ovtcharova M, Schaltegger U, Schmid SM (2011) Cenozoic granitoids in the Dinarides of southern Serbia: age of intrusion, isotope geochemistry, exhumation history and significance for the geodynamic evolution of the Balkan Peninsula. Int J Earth Sci 100(5):1181–1206

Schmid SM, Bernoulli D, Fügenschuh B, Matenco L, Schefer S, Schuster R, Ustaszewski K (2008) The Alpine-Carpathian-Dinaridic orogenic system: correlation and evolution of tectonic units. Swiss J Geosci 101(1):139–183

Selmeczi I (2008) Oligocene (Cenozoic). In: Budai T, Fodor L (ed): Geology of the Vértes Hills. Explanatory book to the Geological Map of the Vértes Hills 1:50000. Geol Inst Hung 258–260

Siegesmund S, Oriolo S, Schulz B, Heinrichs T, Basei MAS, Lammerer B (2021) The birth of the Alps: Ediacaran to Paleozoic accretionary processes and crustal growth along the northern Gondwana margin. Int J Earth Sci 110(4):1321–1348

Sipos-Benkő K, Márton E, Fodor L, Pethe M (2014) An integrated magnetic susceptibility anisotropy (AMS) and structural geological study on Cenozoic clay rich sediments from the Transdanubian Range. Central European Geology 51(1):21–52. https://doi.org/10.1556/CEuGeol.57.2014.1.2

Skopelitis A, Brack P, Ulianov A, Bindeman I, Schaltegger U (2011) Tracing episodic magma accretion by zircon 18O/16O isotopes and U-Pb dating in the Adamello batholith, Italy. Goldschmidt Conference, Prague pp 14–19

Sliwinski JT, Guillong M, Liebske C, Dunkl I, von Quadt A, Bachmann O (2017) Improved accuracy of LA-ICP-MS U-Pb ages of Cenozoic zircons by alpha dose correction. Chem Geol 472:8–21

Smirčić D, Kolar-Jurkovšek T, Aljinović D, Barudžija U, Jurkovšek B, Hrvatović H (2018) Stratigraphic definition and correlation of Middle Triassic volcaniclastic facies in the External Dinarides: Croatia and Bosnia and Herzegovina. J Earth Sci 29(4):864–878

Söllner F, Miller H, Höll R (1997) Alter und Genese rhyodazitischer Metavulkanite. Z Dtsch Geol Ges 148(3–4):499–522

Soták J (2010) Paleoenvironmental changes across the Eocene-Oligocene boundary: insights from the Central-Carpathian Paleogene Basin. Geol Carpathica 61(5):393

Storck JC, Brack P, Wotzlaw JF, Ulmer P (2019) Timing and evolution of Middle Triassic magmatism in the Southern Alps (northern Italy). J Geo Soci 176(2):253–268

Szabó I, Ravasz C (1970) Investigation of the Middle Triassic volcanics of the Transdanubian Central Mountains, Hungary. Ann Hist Nat Mus Nat Hung 62:31–51

Szantner F, Szabó E (1969) The structural geological conditions and history of development of Hungarian bauxite deposits. Ann Geol Inst Hung 54:109–130

Szemerédi M, Lukács R, Varga A, Dunkl I, Józsa S, Tatu M, Pál-Molnár E, Szepesi J, Guillong M, Szakmány G, Harangi S (2020) Permian felsic volcanic rocks in the Pannonian Basin (Hungary): new petrographic, geochemical, and geochronological results. Int J Earth Sci 109(1):101–125

Taeger H (1909) Geology of the Vértes Mountains. Magyar Királyi Földtani Intézet Évkönyve 17:1–256

Tari G (1994) Alpine Tectonics of the Pannonian basin. PhD. Thesis, Rice University, Texas, USA

Tari G, Horváth F (2010) Eo-Alpine evolution of the Transdanubian range in the nappe system of the Eastern Alps: revival of a 15 years old tectonic model. Bull Hung Geol Soc 140(4):483–510

Tari G, Báldi T, Báldi-Beke M (1993) Paleogene retroarc flexural basin beneath the Neogene Pannonian Basin: a geodynamical model. Tectonophysics 226:433–455. https://doi.org/10.1016/0040-1951(93)90131-3

Tari G, Bada G, Beidinger A, Csizmeg J, Danišik M, Gjerazi I, Grasemann B, Kováč M, Plašienka D, Šujan M, Szafián P (2021) The connection between the Alps and the Carpathians beneath the Pannonian Basin: Selective reactivation of Alpine nappe contacts during Miocene extension. Glob Planet Change 197:103–401

Telegdi-Roth K (1927) Traces of an infraoligocene denudation at the northwestern edge of the Transdanubian Range. Bull Hung Geol Soc 57:117–128

Tiepolo M, Tribuzio R, Ji WQ, Wu FY, Lustrino M (2014) Alpine Tethys closure as revealed by amphibole-rich mafic and ultramafic rocks from the Adamello and the Bergell intrusions (Central Alps). J Geol Soc 171:793–799

Trabelsi K, Sames B, Wagreich M, Kázmér M, Mindszenty A, Martín-Closas C (2021) A new diverse charophyte flora and biozonation of the Eocene bauxite cover-sequence at Gánt (Vértes Hills, Hungary). J Syst Palaeontol 19(7):541–563

Van Couvering JA, Aubry MP, Berggren WA, Bujak JP, Naeser CW, Wieser T (1981) The terminal Eocene event and the Polish connection. Palaeo Palaeo Palaeo 36(3–4):321–362

Vermeesch P (2012) On the visualisation of detrital age distributions. Chem Geol 312:190–194

Villa IM, von Blanckenburg F (1991) A hornblende 39Ar–40Ar age traverse of the Bregaglia tonalite (southeast Central Alps). Schweiz Mineral Petrogr Mitt 71:73–87. https://doi.org/10.5169/seals-54347

Vörös I (1958) Micromineralogical and trace element study of selected bauxite profiles from Iszkaszentgyörgy. Bull Hung Geol Soc 88(1):48–56

Vörös A, Galácz A (1998) Jurassic palaeogeography of the Transdanubian Central Range (Hungary). Riv Italiana Di Paleontol Strat 104(1):69–84

Wang Q, Liu X, Yan C, Cai S, Li Z, Wang Y, Zhao J, Li G (2012) Mineralogical and geochemical studies of boron-rich bauxite ore deposits in the Songqi region, SW Henan, China. Ore Geol Rev 48:258–270

Wang R, Wang Q, Huang Y, Yang S, Liu X, Zhou Q (2018) Combined tectonic and paleogeographic controls on the genesis of bauxite in the Early Carboniferous to Permian Central Yangtze Island. Ore Geol Rev 101:468–480

Westerhold T, Marwan N, Drury AJ, Liebrand D, Zachos JC (2020) An astronomically dated record of Earth's climate and its predictability over the last 66 million years. Science 369:1383–1387

Zachos J, Dickens G, Zeebe R (2008) An early Cenozoic perspective on greenhouse warming and carbon-cycle dynamics. Nature 451:279–283

Ziegler PA (1990) Geological Atlas of Western and Central Europe Shell Internationale Petroleum Maatschappij B.V. p 239